Am J Cancer Res 2023;13(9):3963-3982
www.ajcr.us /ISSN:2156-6976/ajcr0151376

Original Article

SLC17A9 as a prognostic biomarker correlated with immune infiltrates in human non-small cell lung cancer

Yan Gao[1,2*], Yijia Chen[1,2*], Min Liu[1,2], Daobing Zeng[1,2], Fan Tan[1,2], Huabing Wan[1,2], Xusheng Liu[1,2], Shanchun Su[1,2], Yaohua Zhang[1,2], Yu Zhang[1,2], Changbin Ke[1,2], Zhijun Pei[1,2,3]

[1]Department of Nuclear Medicine and Institute of Anesthesiology and Pain, Taihe Hospital, Hubei University of Medicine, Shiyan 442000, Hubei, China; [2]Department of Health Management Center, Taihe Hospital, Hubei University of Medicine, Shiyan 442000, Hubei, China; [3]Hubei Key Laboratory of Embryonic Stem Cell Research, Shiyan 442000, Hubei, China. [*]Equal contributors.

Received May 22, 2023; Accepted August 8, 2023; Epub September 15, 2023; Published September 30, 2023

Abstract: The vesicular nucleotide transporter (SLC17A9) has been overexpressed in various cancers. Nonetheless, little is known about its influence on non-small cell lung cancer (NSCLC), including human lung adenocarcinoma (LUAD) and lung squamous cell carcinoma (LUSC). Integrative bioinformatics analysis was performed to investigate the prognostic significance and underlying mechanisms of SLC17A9 in patients with NSCLC. Here, we found that SLC17A9 up-regulation was significantly correlated with overall survival in LUAD and LUSC ($P < 0.05$). Gene set enrichment analysis and protein-protein interaction results revealed that SLC17A9 up-regulation was linked to metabolic process, the hallmark of MYC targets, DNA repair, coagulation and complement. SLC17A9 expression was negatively associated with overall survival and positively related to most LUSC immune cells and immunoinhibitor (20/23), particularly immuno A2aR, PD-1, and CTLA-4 ($P < 0.001$). High SLC17A9 was associated with infiltrating levels of B cells, $CD4^+$ T cells, M1 macrophages, and T cell exhaustion checkpoints such as PD-1, CTLA4, and LAG3 in LUAD. Moreover, Real-time PCR, MTS assay, *EdU* assay, ATP production assays and cell cycle analysis were performed to validate SLC17A9 knockdown in LUAD cells. SLC17A9 knockdown significantly inhibited cell proliferation and ATP levels by affecting P2X1, Cytochrome C, and STAT3 expression in lung cancer cells. In conclusion, the present study suggested that SLC17A9 could potentially serve as a prognostic biomarker and correlated with immune infiltrates in LUAD and LUSC.

Keywords: SLC17A9, prognosis, lung adenocarcinoma, lung squamous cell carcinoma, immune infiltrates

Introduction

Lung cancer is the leading cause of cancer death worldwide, with non-small cell lung cancer (NSCLC) accounting for approximately 85% of all cases. The 5-year survival rate for NSCLC is much higher in the early stage, but only 4.5% for metastatic disease [1]. The most prevalent histopathological subtypes of NSCLC are lung adenocarcinoma (LUAD) and lung squamous cell carcinoma (LUSC). Nevertheless, poor prognosis, identifying early diagnostic biomarkers and treatment options for LUAD and LUSC remain significant clinical challenges [2]. Large-scale genomic studies have revealed molecular features and improved our understanding of the underlying mechanisms of many tumor types, which may explain the associations in survival among patients with different pathological staging [3]. Comprehensive multi-platform analyses may be helpful in prognosis and biomarker screening involved in tumor progression in the early stage of NSCLC [4, 5]. In addition, numerous studies demonstrated that immunotherapy targeting the tumor microenvironment (TME), including cancer cells and innate and adaptive immune cells, is a strategy strongly pursued against human cancers [6]. TME immune checkpoint proteins such as cytotoxic T lymphocyte associated antigen 4 (CTLA4), programmed death-1 (PD-1), and programmed death ligand-1 (PD-L1) inhibit T-cell mediated immune responses in NSCLC [7, 8]. However, it has previously been reported that only a small proportion of NSCLC patients benefit from immune checkpoint inhibitors [9-11].

There is a critical need to identify novel immune related therapeutic targets in NSCLC, so as to better understand and improve treatment strategies.

Solute carrier family 17 (SLC17) proteins are responsible for transporting organic anions across membranes. Nine transmembrane segment transporters (SLC17A1-9) are currently known, including type I phosphate transporters (SLC17A1-4), vesicular glutamate transporters (SLC17A6-8), and a lysosomal acidic sugar transporter (sialin, SLC17A5) [12]. SLC17A9, the most recently described vesicular nucleotide transporter, mediates liposomal ATP accumulation and could regulate cell viability [13, 14] and osteoblast differentiation [15]. SLC17A9 overexpression has been identified in various human cancers, including liver cancer [16, 17], colorectal cancer [18], gastric carcinoma [19], and prostate cancer [20]. SLC17A9 is associated with a poor prognosis in clear cell renal cell carcinoma [21], where it up-regulates the expression of parathyroid hormone like hormone and promotes proliferation, migration, invasion, and drug resistance [22]. Mi *et al*. reported that LINC01679 acts as a competing endogenous RNA that inhibits prostate cancer progression by regulating the miR-3150a-3p/SLC17A9 axis [20]. In addition, SLC17A9 also regulates T cell activation [23], gastrointestinal baroreception, and chronic inflammation [24]. However, a link between SLC17A9 and immune cell infiltration in cancers has been uncovered. Little is known regarding the expression, prognosis and underlying functions of SLC17A9 in NSCLC, which requires further investigation.

In the present study, we analyzed the mRNA expression of all nine subsets of SLC17 using data from The Cancer Genome Atlas (TCGA) database. We investigated the associations of SLC17A9 expression with survival outcomes and immune infiltration in LUAD and LUSC patients. Gene ontology (GO), Kyoto Encyclopedia of Genes and Genomes (KEGG) pathways enrichment, Gene Set Enrichment Analysis (GSEA), and protein-protein interaction (PPI) network of co-expressed genes were performed to determine the mechanism of SLC17A9 in NSCLC patients. In addition, the function and potential mechanisms of SLC17A9 in lung cancer cell growth were also investigated. The findings provide a potential diagnostic and prognostic biomarker for NSCLC.

Materials and methods

Expression analysis by TCGA, GEO, GEPIA2, and cBioPortal database

The mRNA expression profiles (HTSeq FPKM and HTSeq counts) were downloaded from TCGA database (https://portal.gdc.cancer.gov/) and transformed into transcripts per million reads (TPM) +1 for further analysis. The associated clinical data for 510 LUAD, 546 LUSC and normal lung tissue samples were also obtained. The expression profiles of nine SLC17A family genes was plotted in the ggplot2 R [25]. To investigate the differences in SLC17A9 expression between NSCLC and non-cancer samples, the expression profiles of GSE74706, GSE33532, GSE18842, GSE116959, and GSE4127 were downloaded from the Gene Expression Omnibus (GEO) database. The GPL570 platform was used to obtain both GSE18842 and GSE33532. GSE74706, GSE116959, and GSE4127 are derived from the GPL13497, GPL17077, and GPL96 platforms, respectively. Gene Expression Profiling Interactive Analysis 2 (GEPIA2; http://gepia2.cancer-pku.cn/#index) was used to compare gene expression between tumor tissues and match TCGA normal data. To find the genomic profiles of nine SLC17A family members, the location and frequency of SLC17A alterations (amplifications, deep deletions, missense mutations and truncating mutations) and copy number variance data were retrieved from TCGA lung cancer datasets using the online resource cBiopPortal (www.cbioportal.org) [26].

Immunohistochemistry (IHC)

The paraffin-embedded surgical specimens of 30 LUAD patients between February 2018 and September 2019 at Taihe Hospital were retrospectively collected and sectioned for immunohistochemistry. The review boards of the Biomedical Ethics Committee of Taihe Hospital have approved a waiver of consent. The IHC experiment was conducted as described previously [3]. The sectioned tissue was incubated with rabbit anti-SLC17A9 antibody (1:20, Abcam, ab185576) at 4°C overnight. Then the slides were coupled with the rabbit secondary antibody (1:600, Abcam) at room temperature for 1.0 h. IHC results were evaluated by two experienced observers who were blinded to the condition of the patients.

The diagnosis and prognosis analysis of SLC17A members

A Kaplan-Meier analysis was conducted to evaluate gene-associated hazard ratios (HRs) for overall survival (OS) based on RNA-seq and genechip data from GEO and TCGA databases. Kaplan-Meier plots (http://kmplot.com/analysis/) [27] were used to examine the correlation between gene expression and OS rates in LUAD and LUSC patients. Furthermore, the best cut-off point of the gene for survival analysis was ascertain by the "surv cutpoint" function in the "survminer" R package. The survival map of "hub" genes was prepared by GEPIA2 database.

The "pROC" of the R package was used to perform the receiver operating characteristic (ROC) curve analysis with the clinicopathological parameters of TCGA lung cancer. The ROC curve was generated on the true positive ratio (TPR, or sensitivity) and false positive ratio (FPR, or 1-specificity). It was used to calculate the area under the curve (AUC) and evaluate the prognostic or predictive accuracy.

To further investigate the SLC17A9 expression association with other clinical features, 513 LUAD and 501 LUSC patients were divided into high and low groups based on the median value of SLC17A9 expression in TCGA database. The χ^2 square was performed to evaluate the relationship between SLC17A expression and clinicopathological parameters such as TNM stage, age, gender, and OS.

Screening of SLC17A9 co-expressed genes via LinkedOmics database and functional enrichment analysis

The LinkedOmics database (http://www.linkedomics.org/login.php) is a web-based platform for analyzing all 32 TCGA cancer-associated multi-dimensional datasets [28]. SLC17A9 co-expression in LUAD and LUSC was statistically compared using Pearson's correlation coefficient, and presented as heat maps. Subsequently, co-expressed genes were signed and ranked using the GO: BP (biological process), CC (cellular component), MF (molecular function), and KEGG pathway analyses.

Gene set enrichment analysis (GSEA)

GSEA was conducted to identify significant differences between SLC17A9 low and high expression groups in NSCLC using TCGA and GEO databases. The differentially expressed genes in SLC17A9-low (0-25%) and SLC17A9-high (75-100%) expression groups in TCGA database were assessed using the "DESeq2" R package and presented by the ggplot2 [3.3.6] R package. Then the GSEA was conducted by "cluster Profiler" and "msigdbr" R package using gene sets from the c2.cp.all.v2022.1.Hs.symbols.gmt [All Canonical Pathways] (3050) in Molecular Signature Database (MSigDB v7.2). GSEA was also performed using GEO matrix of the GSE18842 (N = 46). The H hallmark gene sets were also downloaded from the molecular signatures database. The NES and nominal *P* value for the GSEA were calculated by a permutation number set at 1000. Enriched gene sets were selected for FDR < 0.05 and NES > 1.50.

PPI network construction

Search Tool for the Retrieval of Interacting Genes/Proteins (STRING) 11.0 (https://string-db.org/) is a database of known and predicted protein interactions that contains both direct and indirect protein associations [29]. SLC17A9 was imported into the STRING database, and PPI analysis with a combined score of > 0.4 was performed. Subsequently, the Cytohubba plugin in Cytoscape was used to calculate the degree of each protein node. Top genes were defined as "hub" genes.

Estimation of immune cell type fractions

The xCell, pheatmap, gene set variation analysis (GSVA), and ssGSEA R packages were utilized for reliable immune cell type enrichment analysis. The Tumor Immune Estimation Resource (TIMER, https://cistrome.shinyapps.io/timer/) database includes 10,897 samples across 32 cancer types from TCGA to illustrate the correlation between two genes using the Spearman correlation coefficient and to estimate statistical significance [30]. It was utilized to estimate the correlations between SLC17A9 and gene marker sets of different types of innate and adaptive immunity. The expression of the immune checkpoint-related genes, including SIGLEC15, IDO1, CD274, HAVCR2, PDCD1, CTLA4, LAG3, and PDCD1LG2, was examined in SLC17A9 high and low groups. The ggplot2 and *pheatmap* R packages were utilized to investigate the relationship between SLC17A9 and immune checkpoints in LUAD and LUSC.

Table 1. Primer sequences for RT-PCR

Target	Forward	Reverse
ACTB	TCTTCCAGCCTTCCTTCCT	AGCACTGTGTTGGCGTACAG
SLC17A9	AGGGGTTTACTTCCCTGCC	GTCAGCAGCGTCCCAAACT
P2RX1	CTACAATGACCACCATCGGCTCTG	CTTAGGCAGGATGTGAAGCAGCAG
MYC	CGCCTCTTGACATTCTCCTC	GGACTATCCTGCTGCCAAGA
Cytochrome C	ATTGGCGGCTGTGTAAGAGT	AAGTGTTCCCAGTGCCACA
MFN2	AGCCCTCGGTAAGGAGAAAG	GTGATCAATGCCATGCTCTG
STAT3	TCGGCTAGAAAACTGGATAACG	TGCAACTCCTCCAGTTTCTTAA

Cell culture and treatment

Human LUAD cell lines A549 and H1299 were purchased from ATCC and cultured in high glucose DMEM (HyClone) supplemented with 10% fetal bovine serum (Gibco). The small interfering RNA (siRNA) targeting human SLC17A9 was synthesized by GenePharma and transfected into the cells using Lipofectamine 8000 reagent (Beyotime). Non-specific siRNA was used as a negative control. The siRNA oligonucleotide sequences are displayed as follows: siSLC17A9-1, Sense 5'-UUUCUGUUAACAUCCAGGATT-3', Antisense 5'-UCCUGGAUGUUAACAGAAAUG-3'. siSLC17A9-2, Sense 5'-CUCUGAUCAUCUCAUCAAUTT-3', Antisense 5'-AUUGAUGAGAUGAUCAGAGTT-3'. siNC, Sense 5'-ACGUGACACGUUCGGAGAA-3', Antisense 5'-UCUUCUCCGAACGUGUCACGU-3'.

RNA isolation and real-time quantitative PCR analysis

Total RNA was extracted using TRIzol reagent (Invitrogen). cDNA was synthesized using the TaqMan Reverse Transcription Reagents kit (TaKaRa) for mRNA analysis. Real-time quantitative PCR analysis was performed with different primer sequences using SYBR Green Master Mix (TaKaRa). The primers used for RT-PCR were shown in **Table 1**.

Cell proliferation detection via MTS and EdU assays

Cell viability and growth rate were assessed at 48, 72, and 96 h after siRNA transfection using MTS Assay Kits (Promega) according to the manufacturer's instructions. A standard immunofluorescence assay protocol was performed using the BeyoClick™ *EdU*-488 assay kit (Beyotime) according to the manufacturer's instructions. In brief, following incubation with 10 μM *EdU* for 2 h, the indicated cells were fixed, permeabilized and stained with the Click Additive Solution and DAPI. The images were acquired using a confocal laser-scanning microscope. The density of *EdU*-positive nuclei was calculated for cell proliferation analysis.

ATP detection assay

An ATP bioluminescent assay kit (Beyotime, China) was used to measure intracellular ATP levels according to the manufacturer's instructions. A549 cells were seeded in 6-well plates and collected 72 h after siRNA transfection. The cellular ATP was extracted using an appropriate buffer, mixed with an ATP detection solution containing luciferase. The bioluminescence was measured using a luminescence plate reader. Total ATP levels were expressed as pmol/μg protein.

Cell cycle analysis

Briefly, cells were collected 72 h after siRNA transfection, fixed with 70% ice cold ethanol at 4°C for 12 h, and stained with propidium iodide (50 μg/mL) for 30 minutes. Cell cycles were detected using the flow FACS Gallios Flow Cytometer (BD Biosciences).

Statistical analysis

SPSS version 24.0 was used for data analysis. The χ^2 square test and Spearman correlation test were performed to assess the relationship between SLC17A expression and clinical features of tumor progression. All data analyses were performed in the Xiantao bioinformatics toolbox (https://www.xiantao.love/products) using packages implemented in the R software (version 4.0.3). The following R packages are implemented by R foundation for statistical computing (version 4.0.3): ggplot2, sur-

vival, survminer, pROC, xCell, GSVA, ssGSEA, and *pheatmap*. The results were expressed as the mean ± standard deviation. Statistical differences between groups were analyzed using the student's t-test or one-way analysis of variance in SPSS version 24.0 statistical software (SPSS, Inc., USA). A two-tailed $P < 0.05$ was considered statistically significant.

Results

SLC17A9 acts as the core gene in SLC17A family members in NSCLC

To explore the potential function of SLC17A family members in NSCLC, the mRNA expression levels of nine SLC17As were determined in the human LUAD and LUSC cases in TCGA database. Only SLC17A9 mRNA expression was significantly up-regulated ($P < 0.001$) in tumor tissues than in normal lung tissues, whereas SLC17A5 expression was significantly lower in both LUAD and LUSC samples. SLC17A1/2/3/4/6/7/8 expression was slightly decreased (fold change < 1.2) in tumor tissues (Figure S1A and S1B). The genetic alteration of SLC17A family genes for LUAD (Figure S2A) and LUSC (Figure S2B) varied from 1.1% to 4.0% for individual genes in the cBioPortal database. The genetic alteration rate was highest in SLC17A9 (4.0%). It also indicates that SLC17A9 overexpression in LUSC and LUAD is primarily caused by gene amplification (Figure S2B). In contrast, there was no amplification of SLC17A8 in LUSC and LUAD. The mutation assessor score of R140L and W216R reached 3.5 (high impact on protein function) in SLC17A1 (Figure S2C). Other missense mutation sites with high scores include SLC17A4 (G211W, L114V and G448V), SLC17A6 (G225E), SLC17A8 (M103I, R444C and P175L), suggesting that they could be important regions for the function.

We further evaluated the expression features of SLC17A9 in NSCLC according to TCGA and GSE74706, GSE33532, GSE18842, and GSE116959. SLC17A9 mRNA significantly increased in LUAD, LUSC and NSCLC compared to normal tissues ($P < 0.05$) (**Figure 1A-E**). Furthermore, the GEPIA2 database demonstrated that SLC17A9 mRNA expression was significantly higher in LUAD ($P < 0.05$), but not significantly in LUSC (**Figure 1F**). IHC results revealed that SLC17A9 protein expression was significantly higher in LUAD tissues than in paracancerous tissue (**Figure 1G** and **1H**). SLC17A9 mRNA expression was also abundant in LUAD and LUSC cell lines, especially higher in LU65 and RERF-LC-AI, compared with other cell lines (GSE4127) (**Figure 1I**). Taken together, these data showed that SLC17A9 was significantly up-regulated in NSCLC.

Up-regulation of SLC17A9 correlated with the prognosis and diagnosis of patients with NSCLC

We subsequently evaluated the prognostic significance of SLC17A family members in NSCLC patients. SLC17A3/7/8/9 expression was associated with poorer OS in 513 LUAD patients ($P < 0.05$) (Figure S3A), and SLC17A1/2/4/6/9 expression was correlated with poorer OS in 501 LUSC patients ($P < 0.05$) (Figure S3B). Other members of this protein family did not show any significant correlation with survival rate. ROC analysis suggested that most of these genes had diagnostic values with corresponding AUC (> 0.5) for distinguishing NSCLC patients from healthy individuals. SLC17A3 (0.750), SLC17A8 (0.766), and SLC17A9 (0.893) showed a moderate value (AUC > 0.7) for distinguishing LUAD patients (Figure S4A). Conversely, SLC17A1 (0.701), SLC17A3 (0.932), SLC17A5 (0.897), SLC17A8 (0.811) and SLC17A9 (0.723) demonstrated a moderate value (AUC > 0.7) for LUSC patients (Figure S4B). These results suggested that SLC17As may play important roles in the development of NSCLC.

Kaplan-Meier survival curve analysis revealed that lower SLC17A9 expression (N = 167) was significantly associated with worse OS and progress free interval in LUAD based on and TCGA database (log-rank test $P < 0.05$, **Figure 2A**). Data from Kaplan-Meier plotter database further confirmed that low SLC17A9 expression predicted worse prognosis in LUAD patients (log-rank *P*-value = 0.0012, Hazard ratio = 0.62), while higher SLC17A9 (ID: 219559_at) expression predicted worse prognosis from GeneChip data (log-rank test $P < 0.05$, Hazard ratio = 1.69, **Figure 2B**). Whereas high SLC17A9 expression (N = 324) was correlated with worse OS and progress free interval in TCGA-LUSC patients (log-rank test $P < 0.05$, **Figure 2C**). A similar result was observed in RNA-seq data of Kaplan-Meier plotter database (log-

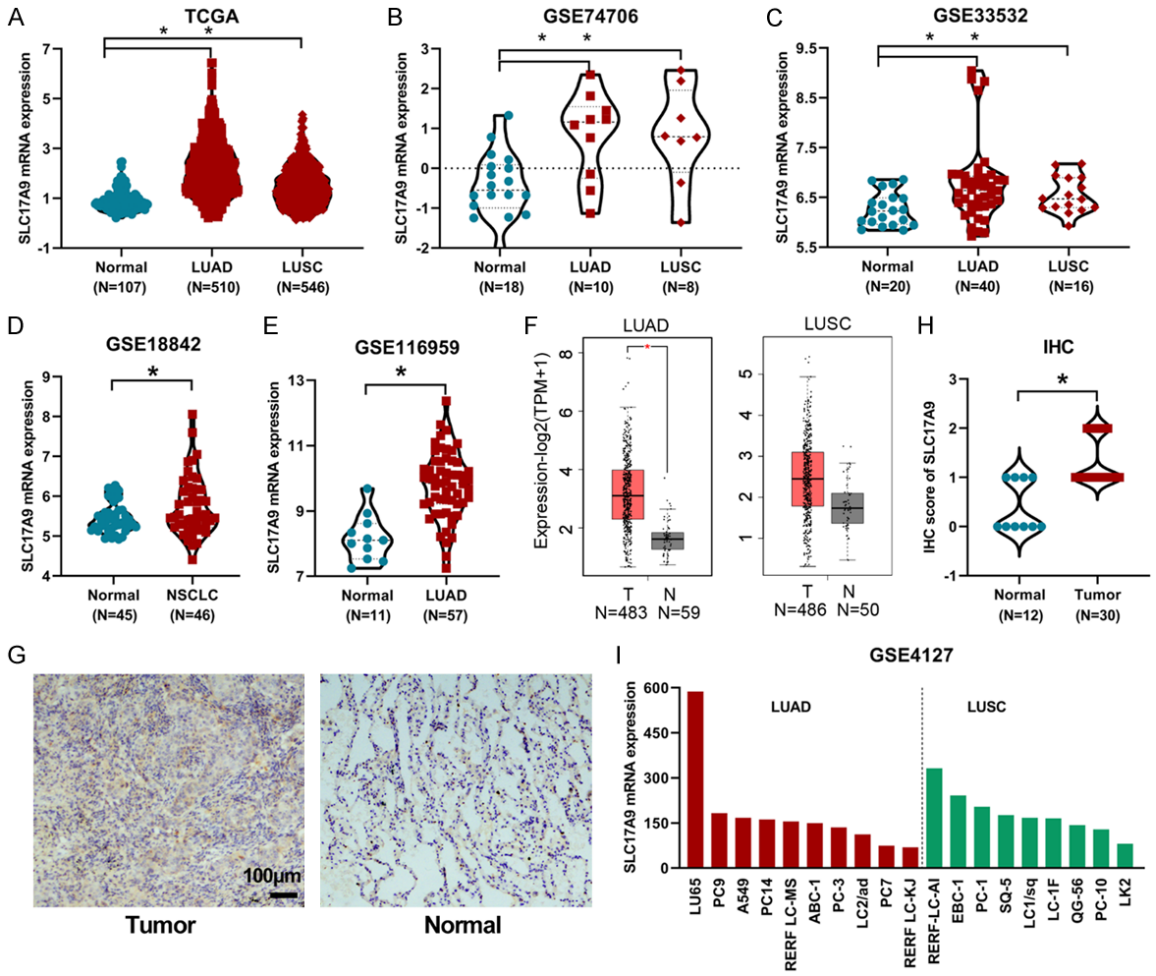

Figure 1. The expression pattern of SLC17A9 in NSCLC and normal tissues. (A) SLC17A9 mRNA expression in tumor tissues and normal tissues from TCGA-LUAD and LUSC cohort (Normal: 109; LUAD: 510; LUSC: 546), GSE74706 (B), GSE33532 (C), GSE18842 (D), GSE116959 (E). (F) Box plots of SLC17A9 expression in LUAD and LUSC and matched TCGA normal tissues based on GEPIA2 datasets. (G) Immunohistochemical staining of SLC17A9 in LUAD tissues (N = 30) and non-tumor tissues (N = 12). (H) Scatterplots of the immunohistochemical staining scores of SLC17A9 expression. (I) SLC17A9 mRNA levels in various LUAD and LUSC cell lines in GEO cohort (GSE4127). *P < 0.05.

rank P-value = 0.024, Hazard ratio = 1.41). High SLC17A9 (232922_s_at) expression from GeneChip data was significantly related to better OS in LUSC (log-rank P-value = 0.04, Hazard ratio = 0.78, **Figure 2D**).

To evaluate the clinical implication of SLC17A9, the relationship between its expression and different clinicopathological parameters was assessed (Table S1). However, SLC17A9 expression was not significantly different by age, gender, stages, and OS in LUAD (N = 502, P > 0.05) and LUSC (P > 0.05). Collectively, SLC17A9 overexpression had the most relevant prognostic and diagnostic value in LUAD and LUSC.

Co-expressed genes and underlying mechanisms of SLC17A9 in LUAD and LUSC

Gene co-expressed with SLC17A9 in the LUAD and LUSC transcriptional data from LinkedOmics were examined to investigate their functional relationship. The heat map indicated the top ten positively and negatively co-expressed genes with SLC17A9 (**Figure 3A** and **3B**). GO and KEGG pathway analyses were performed on the co-expressed genes in both subtypes to reveal the mechanisms. GO term annotation showed that genes co-expressed were primarily involved in biological regulation, metabolic process and protein binding (**Figure 3C**).

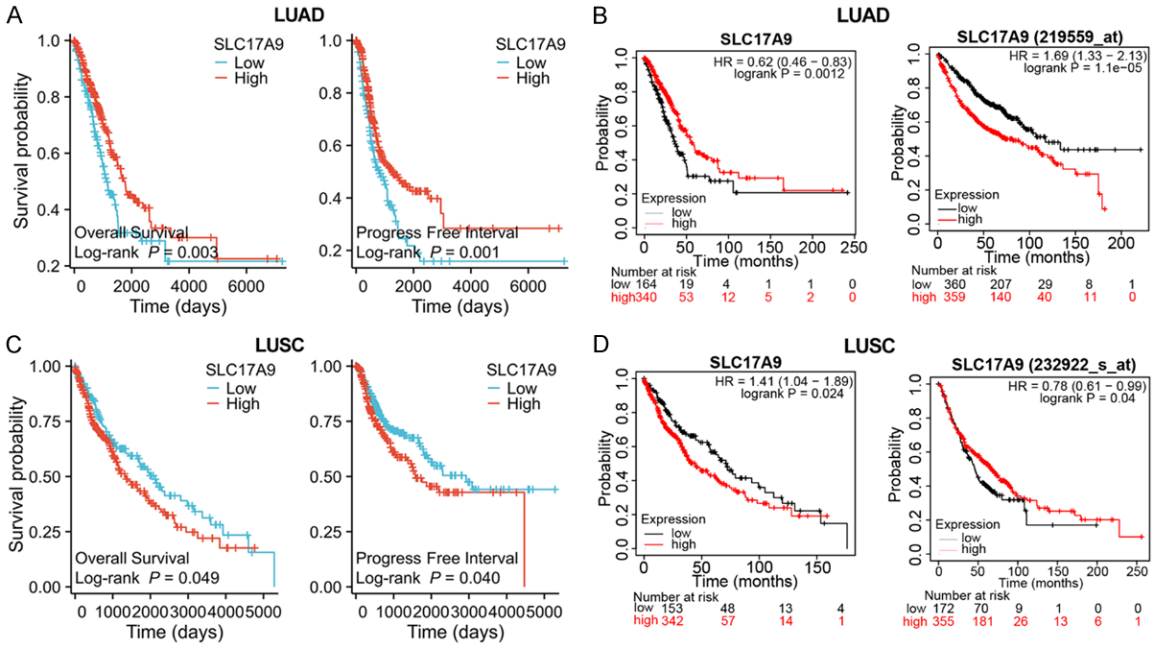

Figure 2. The prognostic value of SLC17A9 in NSCLC. (A) Kaplan-Meier curves for overall survival and progress free interval in LUAD (N = 540) and LUSC (N = 496) (C) patients with high and low expression of SLC17A9 in TCGA database by the "surv_cutpoint" function. (B) Overall survival analysis according to mRNA expression of SLC17A9 in LUAD and LUSC (D) patients using Kaplan-Meier Plotter.

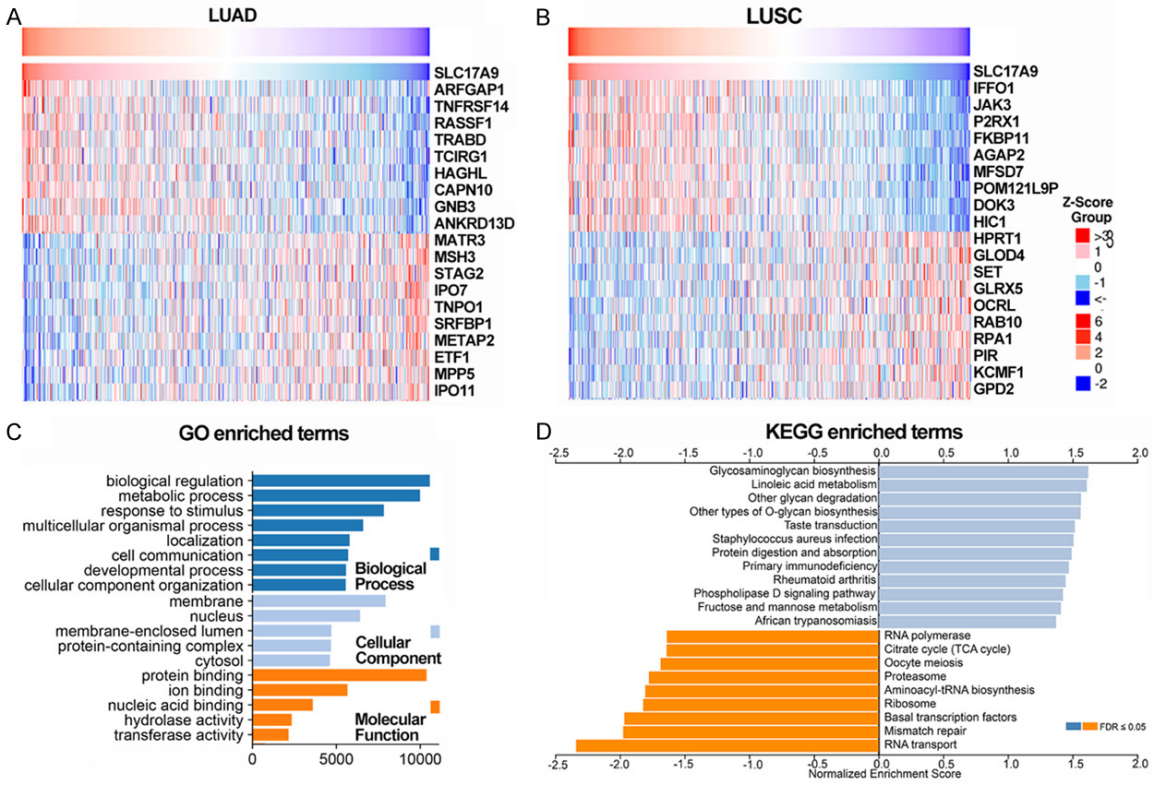

Figure 3. The related signaling pathways associated with SLC17A9 expression levels identified by LinkedOmics. (A) Heat maps showing top 10 genes positively (red) and negatively (blue) correlated with SLC17A9 in LUAD and LUSC (B). (C) The most significantly enriched GO annotations and KEGG pathways (D) identified by comparing LUAD and LUSC.

KEGG analysis revealed that glycosaminoglycan biosynthesis, linoleic acid metabolism, and other glycan degradation were enriched, while RNA transport, mismatch repair, and basal transcription factors were inhibited (**Figure 3D**).

To better understand the potential molecular mechanisms of SLC17A9 in NSCLC, we conducted GSEA analysis on all the differentially expressed genes based on SLC17A9 expression in LUAD (N = 269) and LUSC (N = 251) patients. By the criteria of |LogFC| > 2 & p.adj < 0.05, we identified 1420 differentially expressed genes in LUAD patients with SLC17A9 high expression compared to the SLC17A9 low expression group (**Figure 4A**). There were only 397 differentially expressed genes in LUSC subtype (**Figure 4C**). GSEA of C2 (All Canonical Pathways) results revealed that high SLC17A9 expression was associated with some oncogenic signatures, such as drug metabolism cytochrome P450, biological oxidations, and starch and sucrose metabolism. The DNA methylation, HDACS deacetylate histones, diseases of programmed cell death, and HCMV infection pathways were markedly negatively related to SLC17A9 in LUAD patients (**Figure 4B**). The GSEA analysis revealed that immune-related pathways, such as immunoregulatory interactions between a lymphoid and a non-lymphoid cell, and extrafollicular B cell activation by SARS-CoV-2 signaling pathway were enriched in the SLC17A9 high expression group in LUSC. SLC17A9 was also negatively associated with some essential signaling pathways, such as DNA methylation, metabolism of xenobiotics by cytochrome P450 and DNA_replication in LUSC (**Figure 4D**). Furthermore, GSEA was performed using oncogenic signatures and hallmark gene sets between SLC17A9 high and low expression in 46 NSCLC patients (GSE18842). The top significant hallmark gene sets, including coagulation, complement, MYC targets, and DNA repair, were enriched in the high SLC17A9 expression group (*P < 0.05*, **Figure 4E**).

Potential role of SLC17A9-related hub genes and their prognostic value

To identify the hub genes and understand the relationship between SLC17A9 expression and its potential mechanism in NSCLC, a PPI network with 25 nodes was constructed using the STRING database (**Figure 5A**). SLC17A9, P2RX1, P2RX3, P2RX7, P2RX4, PANX1, WDTC1, ENTPD2, TRIM33, and PANX2 were selected as top 10 hub genes, ranked by degrees of the CytoHubba plugin (**Figure 5B**). To further confirm whether the above hub genes were related to LUAD and LUSC, we analyzed the mRNA expression and prognostic values of the potential hub genes. The analysis demonstrated that these hub genes were significantly altered in LUAD and LUSC patients except for TRIM33 (**Figure 5C**). P2RX1 and WDTC1 expression was associated with the OS of LUAD patients, whereas the high expression of P2X4 and WDTC1 was associated with worse OS in LUSC patients (**Figure 5D**).

Up-regulation of SLC17A9 involved in immune infiltration of patients with LUAD and LUSC

Consistent with previous studies, GSEA analysis showed that high expression of SLC17A9 was involved in immune response [23]. Therefore, we investigated whether SLC17A9 expression correlated with immune infiltration in LUAD and LUSC. The xCell correlation heatmap confirmed that SLC17A9 expression is significantly correlated with most of the $CD8^+$ and $CD4^+$ T cells, plasma B cell, memory B cell, B cells, M1 macrophages and microenvironment score in LUAD ($P < 0.05$, **Figure 6A**). Our GSVA analysis revealed that NK cells, DC cells, Th17, Th1, and Th2 cells were significantly correlated with SLC17A9 expression (**Figure 6B**). Specifically, SLC17A9 expression was associated with most immune infiltrating cells in LUSC (**Figure 7A** and **7B**).

Given the significant role of immune inhibitory or stimulatory genes in tumor therapy, we next selected eight common checkpoint-related genes and various immunoinhibitor genes. We evaluated the correlation of SLC17A9 with these genes using TCGA-LUAD and TCGA-LUSC datasets. The expression of CTLA4, LAG3, PDCD1 (also known as PD-1) and TIGIT was significantly elevated along with high SLC17A9 expression in patients with LUAD ($P < 0.05$, **Figure 6C**). The same was true for HAVCR2, PDCD1LG2, and SIGLEC15 in LUSC ($P < 0.05$, **Figure 7C**).

Additionally, the study revealed that SLC17A9 expression was positively correlated with multiple immunoinhibitors genes, such as A2aR, CD272, CD160, CTLA-4, KIR2DL1, LAG3, LGALS9, PD-1, CD112, TGFB1, TIGIT and B7-H4

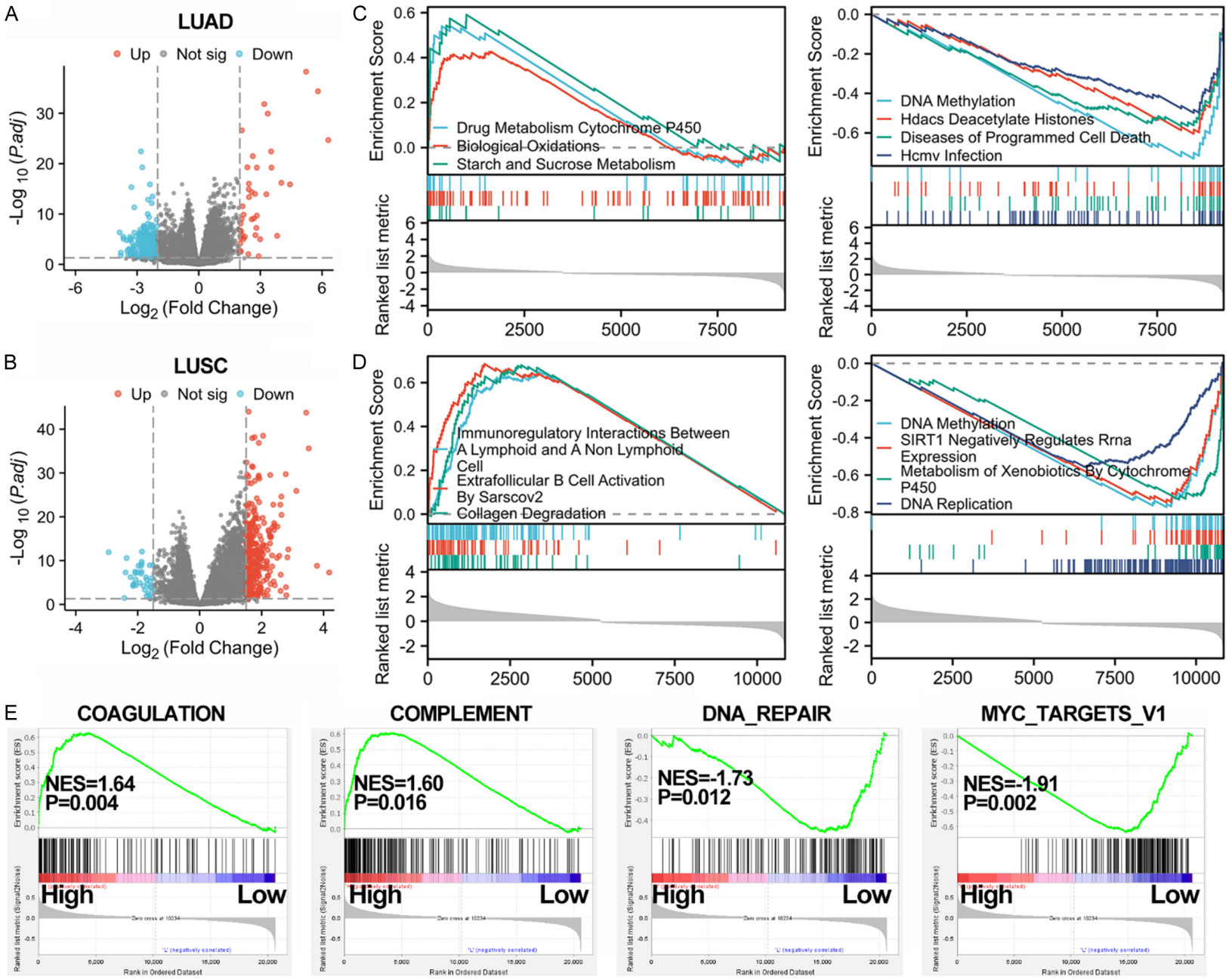
A
LUAD
Up
Not sig
Down
-Log 10 (P.adj)
Log2 (Fold Change)
B
LUSC
C
Enrichment Score
Drug Metabolism Cytochrome P450
Biological Oxidations
Starch and Sucrose Metabolism
Ranked list metric
DNA Methylation
Hdacs Deacetylate Histones
Diseases of Programmed Cell Death
Hcmv Infection
D
Immunoregulatory Interactions Between A Lymphoid and A Non Lymphoid Cell
Extrafollicular B Cell Activation By Sarscov2
Collagen Degradation
SIRT1 Negatively Regulates Rrna Expression
Metabolism of Xenobiotics By Cytochrome P450
DNA Replication
E
COAGULATION
NES=1.64
P=0.004
COMPLEMENT
NES=1.60
P=0.016
DNA_REPAIR
NES=-1.73
P=0.012
MYC_TARGETS_V1
NES=-1.91
P=0.002
High
Low
Rank in Ordered Dataset

Figure 4. Identification of SLC17A9-related signaling pathways by GSEA. (A) Volcano plot showing differentially expressed genes between SLC17A9 high and low expression groups in LUAD patients (N = 269, |LogFC| > 2 and p.adj < 0.05) and in LUSC patients (N = 251, |LogFC| > 1.5 and p.adj < 0.05) (B), the group cutoff points were 25% (high) and 75% (low). (C) Enrichment plots generated by GSEA using gene sets of C2 (All Canonical Pathways) in LUAD and LUSC (D). (E) The strong correlation between SLC17A9 and coagulation, complement, DNA repair and myc targets in the GSEA/Hallmark category (GSE18842). ES, enrichment score; NES, normalized ES; NOM p-val, normalized *p*-value.

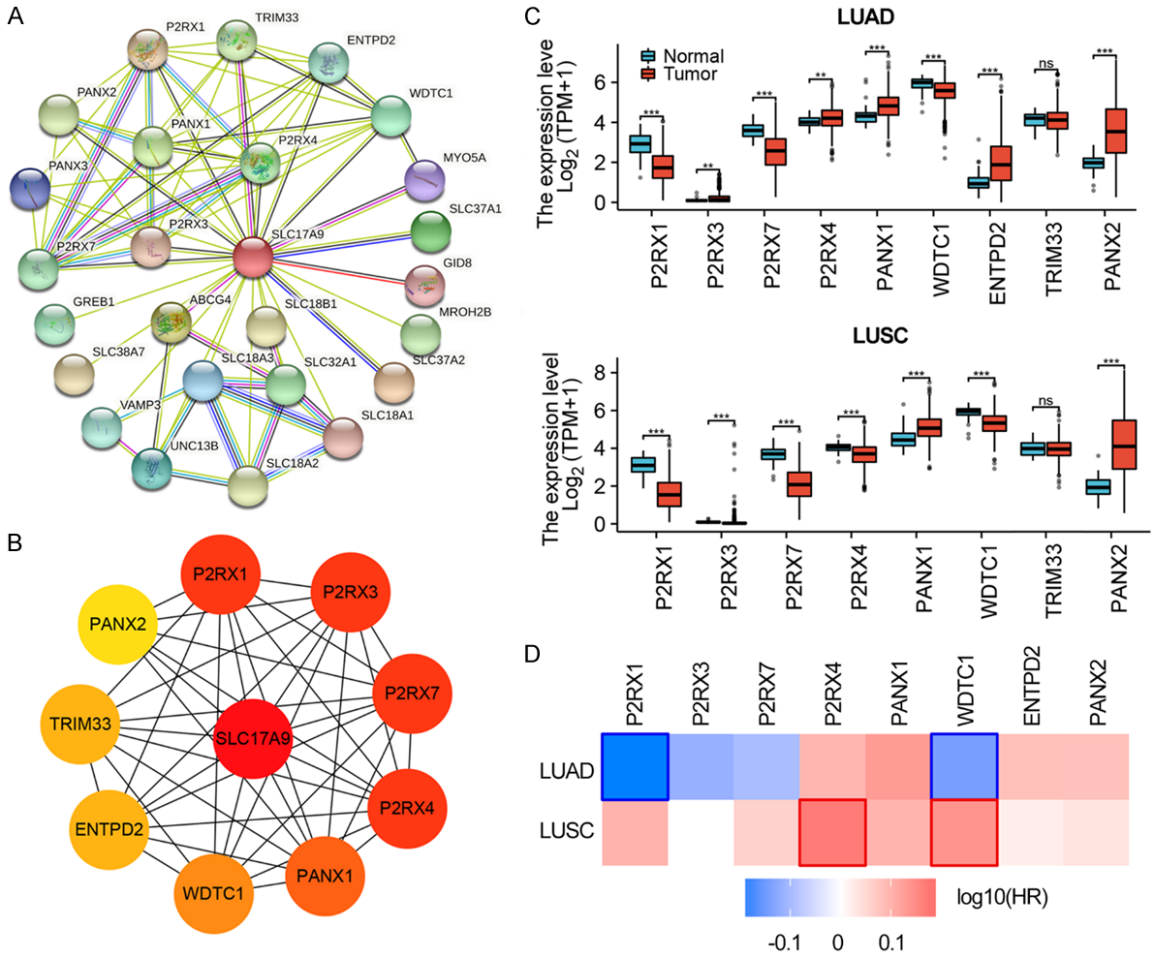

Figure 5. Protein-protein interaction (PPI) network and hub genes analysis. A. PPI network constructed by STRING database for SLC17A9-related gene. B. Ten hub genes in the PPI screened using the cytoHubba module of Cytoscape (higher color represents stronger connectivity). C. Expression levels of the hub genes based on TCGA data, **P* < 0.05, ***P* < 0.01, ****P* < 0.001. D. Overall survival map of hub genes in LUAD (N = 483) and LUSC (N = 486) by GEPIA2 database indicated that P2RX1 and WDTC1 were associated with prognosis in LUAD, high expression of P2RX4 and WDTC1 predicted an unfavorable prognosis in LUSC.

in LUAD (*P* < 0.05, **Figure 6D**). SLC17A9 expression had a strong positive correlation with most immunoinhibitor (21/24) in LUSC, especially with A2aR (r = 0.49, *P* < 0.001), PD-1 (r = 0.43, *P* < 0.001), CTLA-4 (r = 0.41, *P* < 0.001), CSF1R (r = 0.39, *P* < 0.001), and TIGIT (r = 0.37, *P* < 0.001). But SLC17A9 was negatively correlated with B7-H4 (r = -0.10, *P* < 0.05) (*P* < 0.05, **Figure 7D**). These results indicated that SLC17A9 plays a specific role in immune infiltration in LUAD and LUSC, especially for T cells and B cells, and may serve as an immunotherapy target in LUSC.

Correlation analysis between SLC17A9 expression and immune marker sets of patients with LUAD and LUSC

The relationship between SLC17A9 and the immune marker sets of various immune infil-

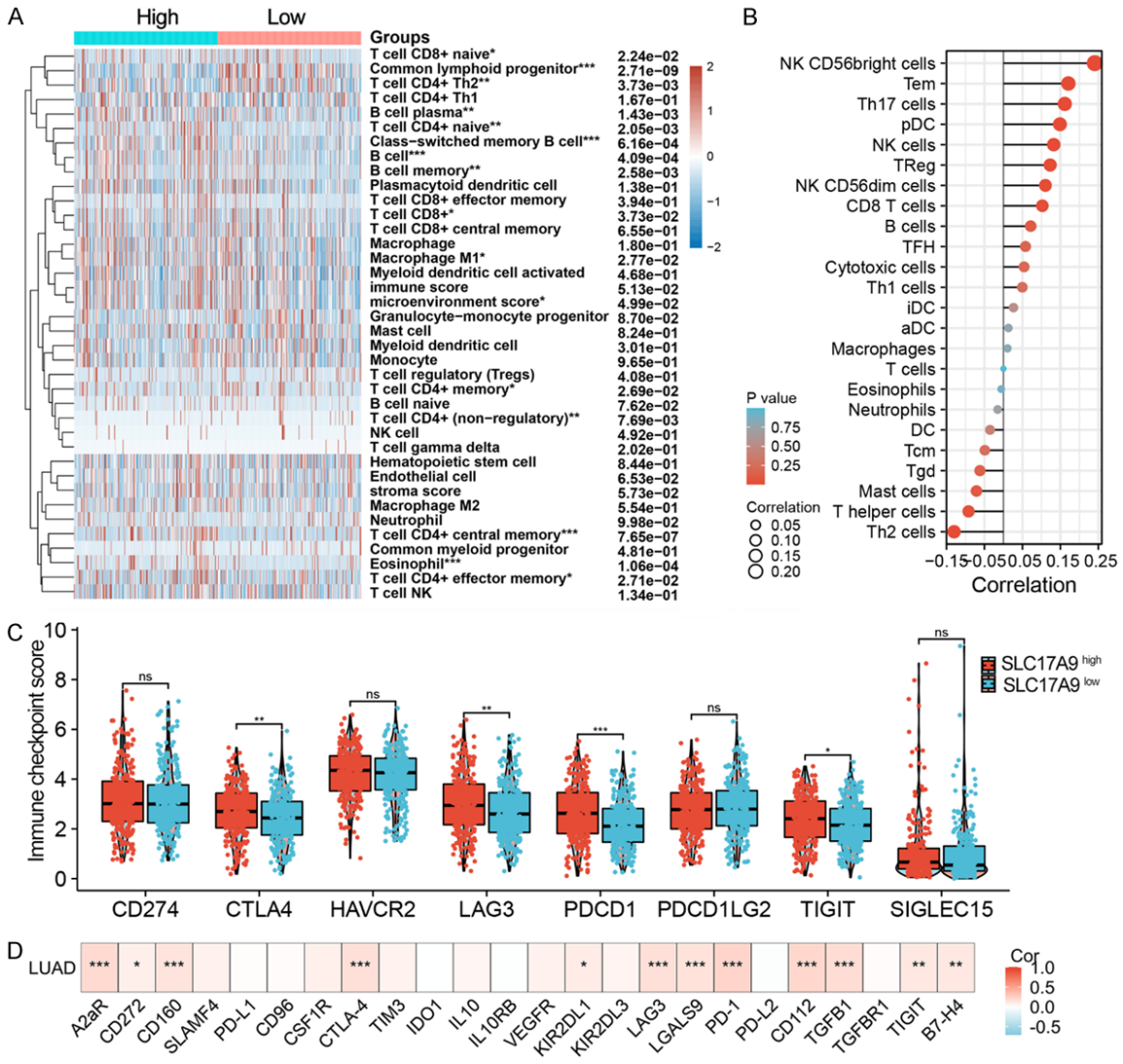

Figure 6. Correlation analysis of SLC17A9 expression with immune infiltration level in LUAD. A. Heatmap depicting the relationship between tumor infiltrating immune cells and SLC17A9 expression levels in each sample. B. Lollipop diagram and bar charts showing the association between tumor infiltrating immune cells and SLC17A9 expression status using GSVA R package. C. Violin plot of immune checkpoints related genes in TCGA-LUAD tumor tissues with high (N = 267) or low (N = 266) SLC17A9 expression. D. The co-expression heatmaps between SLC17A9 expression and immunoinhibitor genes in LUAD by TIMER2.0 and ggplot2 [3.3.6], the color indicates the correlation coefficient. *P < 0.05, **P < 0.01, ***P < 0.001.

trating cells was then investigated in LUAD and LUSC using the TIMER database. The SLC17A9 expression level was significantly correlated with gene markers of innate immunity cells, including CD14 of monocytes, CD68 of tumor-associated macrophages, INOS and TNF-α of M1 macrophages, KIR2DL1, KIR3DL1, KIR3DL3, and KIR2DS4 of Natural killer cells, as well as CD11c and HLA-DQB1 of dendritic cells (P < 0.05, **Table 2**). Marker sets of adaptive immunity cells, including general T cell markers (CD3D and CD3E), B cell markers (CD19, CD20 and CD23), Th1 markers (T-bet and TNF-α), Th2 markers (STAT6, STAT5A and IL13), Tfh marker (CD278), Th17 marker (IL17A), Treg (FOXP3, CCR8, STAT5B, and TGFβ), and T cell exhaustion (PD-1, CTLA4, and LAG3) have strong correlations with SLC17A9 expression in LUAD (P < 0.05, **Table 3**). Interestingly, SLC17A9 expression was significantly correlated with most innate and adaptive immune marker sets in LUSC (P < 0.05, **Table 2**). It revealed that purity adjustment had little effect on these association. SLC17A9 was significantly associ-

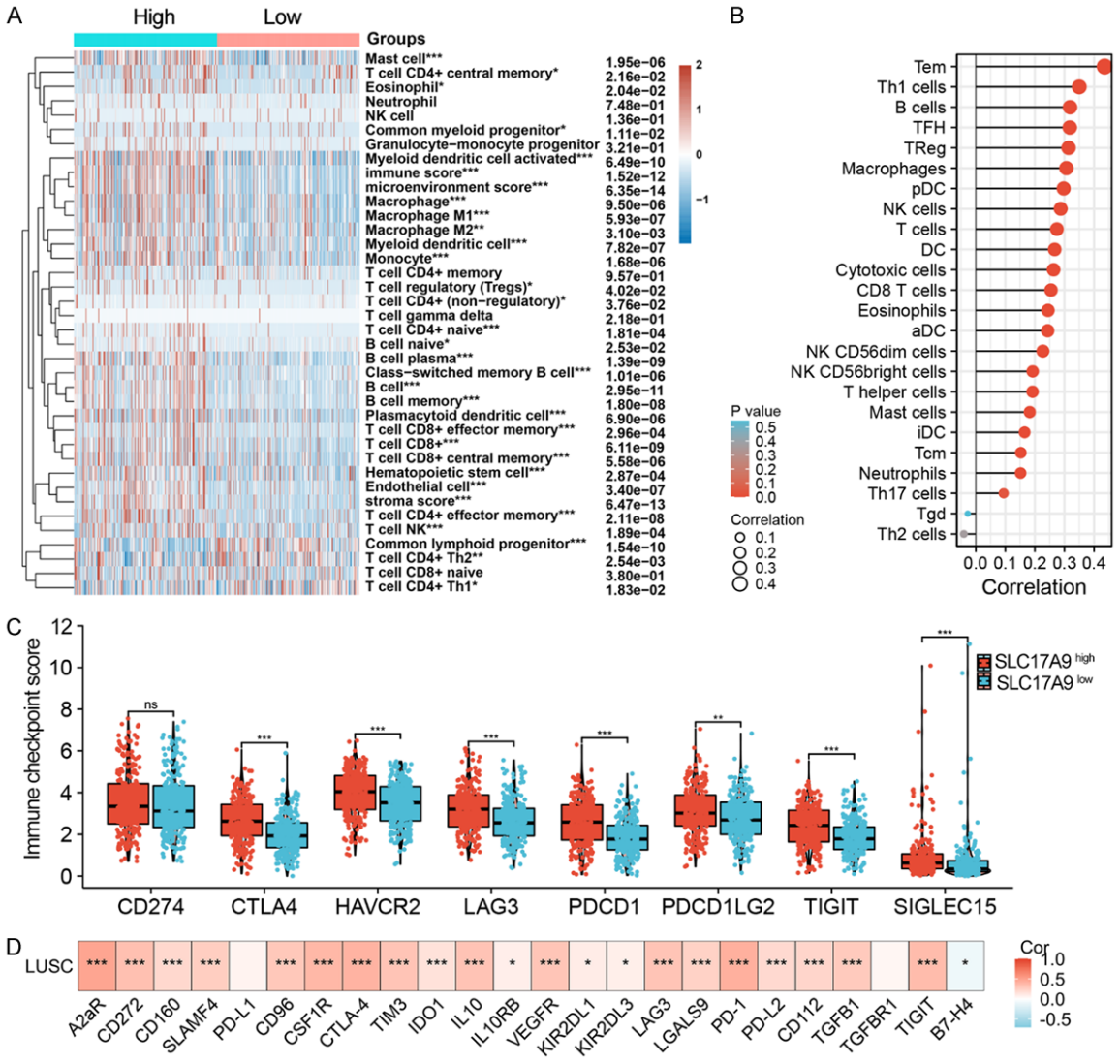

Figure 7. The landscape of immune infiltration drawn by SLC17A9 expression in LUSC. (A) Heatmap and lollipop diagram (B) illustrating the relationship between tumor infiltrating immune cells and SLC17A9 expression in each sample in TCGA database. (C) Expression of immune checkpoints related genes in TCGA-LUSC tumor tissues with high (N = 251) or low (N = 250) SLC17A9 expression. (D) The co-expression heatmaps between SLC17A9 expression and immunoinhibitor genes in LUSC by TIMER2.0 and ggplot2 [3.3.6], the color indicates the correlation coefficient. **P* < 0.05, ***P* < 0.01, ****P* < 0.001.

ated with the expression of immune-related genes in LUSC and LUAD, especially in LUSC, which was consistent with the GSEA results.

Knockdown of SLC17A9 inhibited cell proliferation of lung cancer cells in vitro

To further verify the oncogenic role of SLC17A9 in lung cancer, we examined the effects of SLC17A9 knockdown on the human lung cancer cell lines A549 and H1299. The results showed that both SLC17A9 siRNAs successfully decreased the mRNA expression of SLC17A9, compared to control (**Figure 8A**). MTS assays revealed that the cell proliferation rate of lung cancer cells was inhibited significantly upon SLC17A9 knockdown (**Figure 8B**). The results of *EdU* assays further confirmed that down-regulation of SLC17A9 suppressed cell proliferation (**Figure 8C**). Silencing SLC17A9 expression significantly inhibited lung cancer cell colony formation (**Figure 9A** and **9B**). In the cell cycle analyses, knockdown of SLC17A9 induced G1 arrest and decreased the numbers of A549 cells in the S phase (**Figure 9C**). Furthermore, a decrease in ATP concentration was observed in

Table 2. Correlation analysis between SLC17A9 and relate genes and markers of innate immunity cells in TIMER

Description	Gene markers	LUAD (N = 515)				LUSC (N = 501)			
		Purity		None		Purity		None	
		Cor	*P*	Cor	*P*	Cor	*p*	Cor	*P*
Monocyte	CD14	0.155	*	0.145	*	0.377	*	0.380	*
	CD86	0.082	0.068	0.066	0.133	0.322	*	0.324	*
	CD16 (FCGR3A)	0.050	0.269	0.045	0.311	0.300	*	0.308	*
TAM	CD68	0.112	*	0.106	*	0.241	*	0.251	*
	CCL2	0.075	0.096	0.075	0.088	0.303	*	0.307	*
	CCL5	0.022	0.619	0.022	0.617	0.306	*	0.318	*
M1 macrophage	INOS (NOS2)	0.145	*	0.130	*	0.062	0.175	0.054	0.226
	CXCL10	-0.013	0.770	-0.015	0.741	0.168	*	0.179	*
	TNF-α (TNF)	0.153	*	0.134	*	0.356	*	0.355	*
M2 macrophage	CD206 (MRC1)	0.014	0.750	-0.011	0.798	0.343	*	0.331	*
	CD163	0.082	0.069	0.068	0.122	0.346	*	0.347	*
	IL10	0.069	0.126	0.054	0.218	0.319	*	0.325	*
Neutrophils	CD66b (CEACAM8)	-0.085	0.059	-0.109	*	0.064	0.163	0.075	0.095
	CD11b (ITGAM)	0.133	*	0.115	*	0.430	*	0.424	*
	CCR7	0.143	*	0.125	*	0.404	*	0.406	*
	CD15 (FUT4)	0.149	*	0.164	*	0.324	*	0.332	*
Natural killer cell	KIR2DL1	0.109	*	0.104	*	0.077	0.095	0.103	*
	KIR2DL3	0.068	0.131	0.059	0.182	0.082	0.073	0.089	*
	KIR2DL4	0.056	0.215	0.062	0.161	0.085	0.063	0.106	*
	KIR3DL1	0.108	*	0.093	*	0.171	*	0.183	*
	KIR3DL2	0.048	0.290	0.048	0.274	0.099	*	0.113	*
	KIR3DL3	0.127	*	0.115	*	0.021	0.640	0.045	0.320
	KIR2DS4	0.093	*	0.080	0.071	0.143	*	0.155	*
Dendritic cell	HLA-DPB1	0.038	0.399	0.029	0.512	0.355	*	0.360	*
	HLA-DQB1	0.100	*	0.086	0.052	0.302	*	0.302	*
	HLA-DRA	-0.028	0.531	-0.041	0.356	0.307	*	0.314	*
	HLA-DPA1	0.000	0.998	-0.009	0.845	0.337	*	0.341	*
	BDCA-1 (CD1C)	0.040	0.373	0.022	0.616	0.197	*	0.193	*
	BDCA-4 (NRP1)	-0.028	0.531	-0.038	0.387	0.325	*	0.328	*
	CD11c (ITGAX)	0.314	*	0.303	*	0.518	*	0.517	*
	NKp46 (NCR1)	0.070	0.119	0.068	0.124	0.257	*	0.263	*

TAM, tumorassociated macrophage; Cor, R value of Spearman's correlation; None, correlation without adjustment. Purity, correlation adjusted by purity. *$P < 0.05$.

the SLC17A9 knockdown group (**Figure 9D**). SLC17A9 knockdown significantly increased the mRNA expression of MYC and cytochrome C, but decreased the mRNA expression of the P2X1 receptor, MFN2, and STAT3 compared to control (**Figure 9E**). These findings suggest that knockdown of SLC17A9 inhibited cell proliferation by up-regulation of MYC and cytochrome C and down-regulation of P2X1 receptor, MFN2, and STAT3 in lung cancer cells.

Discussion

The involvement of the SLC17 family of membrane transporters has been reported in various cancers, including colorectal cancer [18], gastric carcinoma [19], hepatocellular carcinoma [16], and acute myeloid leukemia [31]. However, few studies have evaluated the expression pattern and prognosis value of SLC17As in NSCLC. The present study compre-

Table 3. Correlation analysis between CAPRIN1 and relate genes and markers of adaptive immunity cells in TIMER

Description	Gene markers	LUAD (N = 515)				LUSC (N = 501)			
		Purity		None		Purity		None	
		Cor	*P*	Cor	*P*	Cor	*P*	Cor	*P*
$CD8^+$ T cell	CD8A	0.031	0.489	0.028	0.527	0.253	*	0.263	*
	CD8B	0.063	0.159	0.057	0.193	0.228	*	0.234	*
T cell (general)	CD3D	0.098	*	0.089	*	0.319	*	0.332	*
	CD3E	0.101	*	0.096	*	0.362	*	0.369	*
	CD2	0.086	0.057	0.076	0.087	0.341	*	0.350	*
B cell	CD19	0.246	*	0.243	*	0.445	*	0.450	*
	CD20 (MS4A1)	0.171	*	0.162	*	0.332	*	0.337	*
	CD138 (SDC1)	0.046	0.309	0.049	0.263	-0.146	*	-0.152	*
	CD23 (FCER2)	0.169	*	0.155	*	0.326	*	0.323	*
Th1	T-bet (TBX21)	0.171	*	0.164	*	0.400	*	0.411	*
	STAT4	0.070	0.122	0.069	0.117	0.411	*	0.420	*
	STAT1	-0.002	0.969	-0.003	0.953	0.176	*	0.194	*
	IFN-γ (IFNG)	0.056	0.217	0.045	0.313	0.150	*	0.165	*
	TNF-α (TNF)	0.153	*	0.134	*	0.356	*	0.355	*
Th2	GATA3	0.061	0.177	0.059	0.182	0.349	*	0.345	*
	STAT6	0.158	*	0.149	*	0.158	*	0.162	*
	STAT5A	0.226	*	0.216	*	0.432	*	0.440	*
	IL13	0.122	*	0.107	*	0.119	*	0.124	*
Tfh	BCL6	0.081	0.072	0.082	0.064	0.019	0.681	0.005	0.906
	IL21	0.060	0.183	0.042	0.346	0.195	*	0.194	*
	CD278 (ICOS)	0.093	*	0.080	0.069	0.362	*	0.370	*
	CXCL13	0.085	0.060	0.090	*	0.320	*	0.316	*
Th17	STAT3	0.022	0.627	0.020	0.647	0.173	*	0.174	*
	IL17A	0.131	*	0.124	*	0.043	0.348	0.048	0.288
Treg	FOXP3	0.182	*	0.173	*	0.426	*	0.430	*
	CCR8	0.091	*	0.076	0.085	0.353	*	0.358	*
	STAT5B	0.114	*	0.102	*	0.195	*	0.200	*
	TGFβ (TGFB1)	0.181	*	0.185	*	0.293	*	0.288	*
	CD25 (IL2RA)	0.047	0.292	0.038	0.390	0.313	*	0.324	*
T cell exhaustion	PD-1 (PDCD1)	0.231	*	0.229	*	0.420	*	0.430	*
	CTLA4	0.183	*	0.171	*	0.405	*	0.413	*
	LAG3	0.172	*	0.170	*	0.309	*	0.320	*
	TIM-3 (HAVCR2)	0.086	0.057	0.069	0.117	0.314	*	0.322	*
	GZMB	0.088	0.050	0.088	*	0.250	*	0.262	*

Cor, R value of Spearman's correlation; None, correlation without adjustment. Purity, correlation adjusted by purity. *$P < 0.05$.

hensively depicted the expression pattern, mutation, prognostic values, and diagnostic values of SLC17As using LUAD and LUSC samples to identify the key genes. As revealed by our study, most SLC17As were slightly downregulated in human LUAD and LUSC, SLC17A9 mRNA and protein expression significantly upregulated, whereas SLC17A5 expression was significantly lower in tumor tissues of both LUAD and LUSC samples. Genetic mutations (such as missense and truncating mutations) in SLC17As occur frequently and usually cause phenotypic changes, which were associated with human NSCLC [13, 32]. Previous studies have described and identified several disease-causing mutations in SLC17As. The genetic alteration rate was highest in SLC17A9 (4.0%), and the amplification is the most common

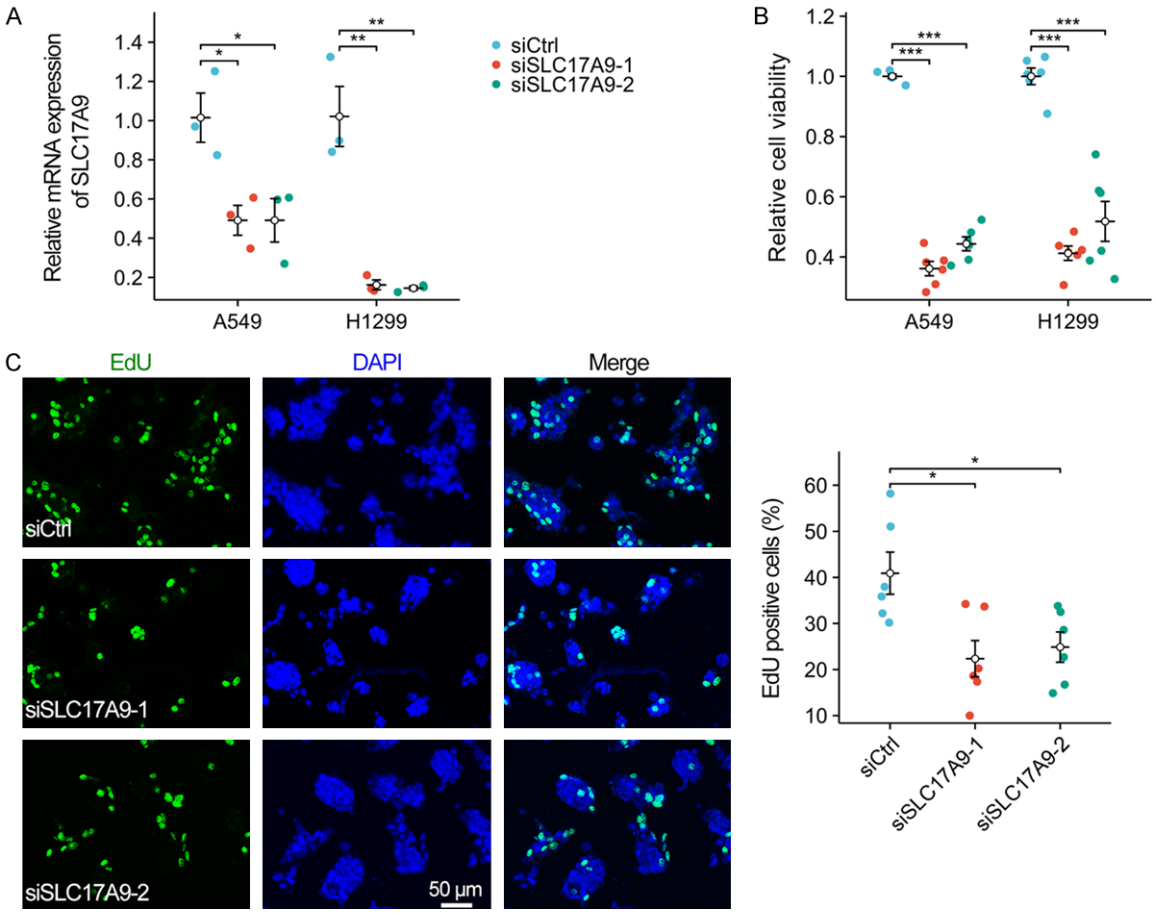

Figure 8. Down-regulation of SLC17A9 inhibited lung cancer cell proliferation. A. Real time PCR analysis of SLC17A9 mRNA expression in A549 and H1299 cells after 48 h of siRNA treatment. B. Cell growth was determined in A49 and H1299 cell lines by MTS assay after SLC17A9 knockdown. C. *EdU* staining of A549 cells and quantification by Image J. $*P < 0.05$, $**P < 0.01$, $***P < 0.001$.

alteration in cancers. SLC17A9 (G78R) was identified as a novel somatic gene mutation in early NSCLC [33], but no other mutations in SLC17A2/3/4/8 were reported. There may also exist associations between SLC17As expression and NSCLC prognosis. It revealed that most SLC17As may be used as diagnostic biomarkers for distinguishing LUAD or LUSC patients from healthy individuals based on ROC analysis. However, we did not find a significant correlation between SLC17A5 expression levels and prognosis in human LUAD and LUSC. Therefore, differentially expressed SLC17A9 was chosen for further investigation in LUAD and LUSC.

Increased expression of SLC17A9 was reported to be associated with poorer survival in patients with prostate cancer [20], clear cell renal cell carcinoma [21], and gastrointestinal cancer including gastric [19], liver [17], and colorectal cancers [18]. Consistent with these findings, we observed that only the mRNA levels of SLC17A9 were significantly higher in human LUAD and LUSC, compared to adjacent normal tissues in TCGA and GEO databases. Additionally, lower expression of SLC17A9 was associated with worse prognosis for LUAD patients in TCGA database. However, SLC17A9 up-regulation was demonstrated as an unfavourable prognostic factor for patients with LUSC. This evidence suggests that the role of SLC17A9 in NSCLC may be specific to the histological subtype. Although adenocarcinoma and squamous cell carcinoma of the lung both derive from the same organ, the tumor biology, patient outcomes, and response to therapy are clearly different in many ways [34]. In addition, the prognosis value of SLC17A9 was different between TCGA data and genechip data of

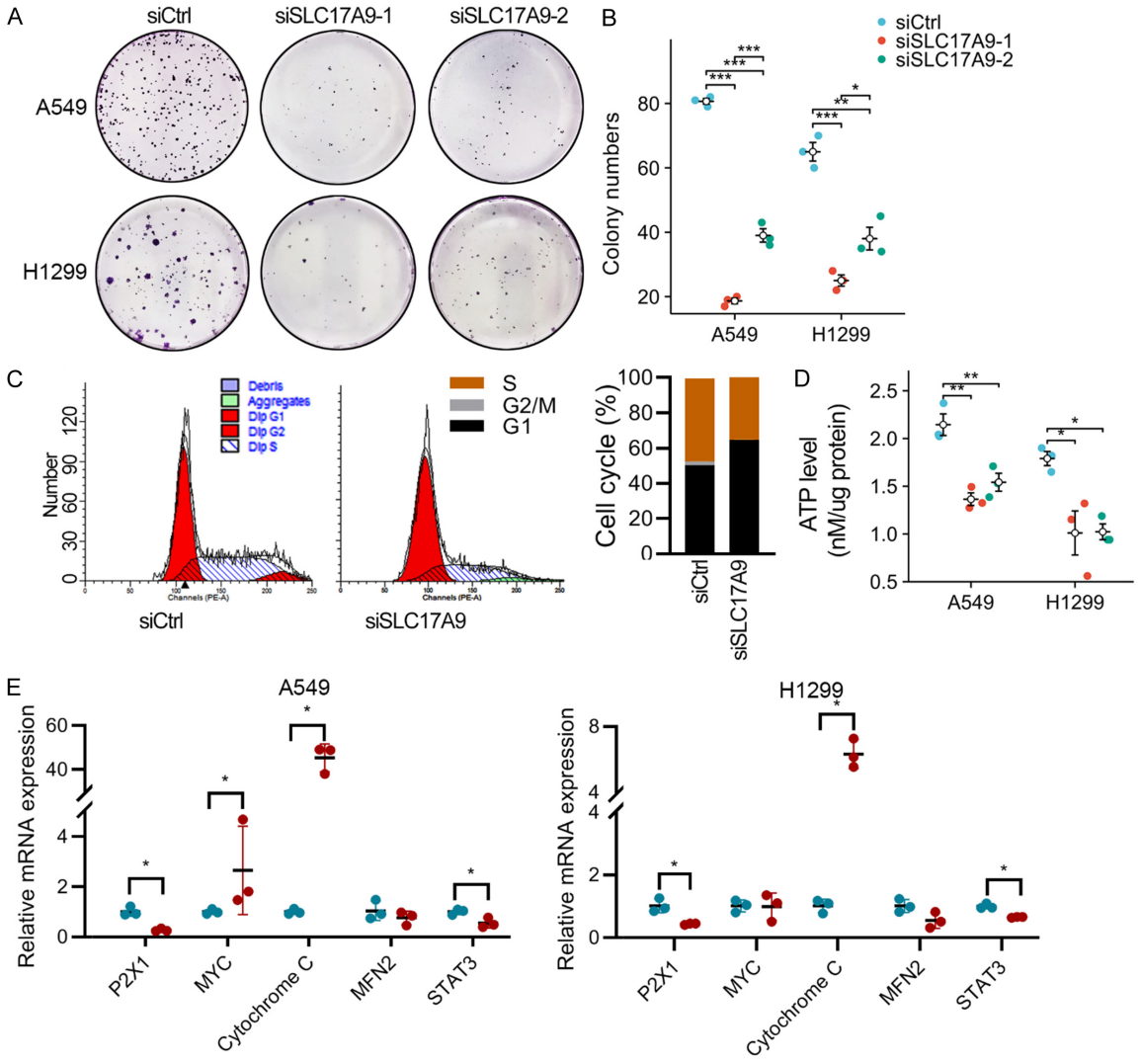

Figure 9. Down-regulation of SLC17A9 inhibited cell proliferation through up-regulation of MYC and cytochrome C. (A) Cell proliferation was determined by colony formation assay and quantification analysis (B). (C) Cell cycle distribution analysis by flow cytometry in A549 cells transfected with SLC17A9 siRNA or control oligos. (D) ATP levels in A549 and H1299 cells after 48 h of siRNA treatment. (E) Real time PCR analysis of P2X1, MYC, cytochrome C, MFN2, and STAT3 in SLC17A9 siRNA transfected cells or control cells. *$P < 0.05$, **$P < 0.01$, ***$P < 0.001$.

Kaplan-Meier plotter database. Different algorithms in different databases may produce the different results. Moreover, the immune function and genetic mutation frequency of SLC17A9 may explain some discrepancies between our analysis and empirical results.

To investigate the oncogenic mechanism of SLC17A9, we analyzed the SLC17A9 co-expression network in LUAD and LUSC using TCGA data. Our findings suggested that the functions of SLC17A9 mainly included biological regulation, metabolic processes (such as glycosaminoglycan biosynthesis and linoleic acid metabolism), and protein binding, while inhibiting RNA transport and mismatch repair. These results were further validated via GSEA, which revealed that oncogenic signaling pathways, such as drug metabolism cytochrome P450, biological oxidations, starch and sucrose metabolism, diseases of programmed cell death and hallmark of MYC targets, DNA repair, coagulation, and complement were related to SLC17A9 up-regulation in NSCLC patients. All these pathways were implicated in cancer cell growth and proliferation [35, 36]. SLC17A9 mRNA expression reportedly correlated positively with a TP53 mutation that could modulate DNA dam-

age response, RNA transport, and protein binding [37]. Recent studies have revealed that SLC17A9 acted as an essential component for vesicular ATP release [38]. ATP could interact with the inotropic P2X1-7 receptors and the metabotropic P2Y1-14 receptors [39]. Zhong *et al*. provided a regulatory mechanism, which suggested that SLC17A9 could transport ATP into the lysosome and activate liposomal P2X4 [40]. Consistent with previous studies, hub genes such as P2RX1, P2RX3, P2RX7, and P2RX4, which were receptors for ATP that acted as a ligand-gated ion channel, were identified with a higher node degree in the PPI network. In recent studies, ATP receptors have also been closely associated with diseases in central nervous system [41] and different tumors [42, 43]. Chong *et al*. [44] demonstrated that mRNA expression of P2X receptor members including P2X1, P2X4, P2X5, and P2X7 increased in Chinese pediatric acute leukemia patients versus controls. In fact, P2X7 activation potentially augmented breast and LUAD-derived A549 invasiveness [45]. We also showed that dysregulation of P2RX1 and WDTC1 was correlated with poor prognosis in patients with LUAD. The mRNA levels of P2RX4 and WDTC1 were significantly lower and related to poor survival for LUSC patients.

In general, the NSCLC TME played a key role in tumor progression and metastasis [46]. A previous study demonstrated that SLC17A9 involved in T cell receptor (TCR)-dependent ATP release [23], which could enhance anti-tumor immunity and the therapeutic efficacy [47-49]. Our GSEA analysis further reported that immune-related pathways were enriched in SLC17A9 high group in LUSC. In the study, we investigated the relationship between SLC17A9 expression and immune cell infiltration levels in the TCGA-LUAD and LUSC tumor samples. We found that SLC17A9 had a strong association with most gene markers and a large population of immune cells in LUSC, including immune checkpoint-related genes, supporting the observation that OS of SLC17A9 lower expression group was significantly worse verse to high expression group. In addition, SLC17A9 was closely related to partial B cells and $CD8^+$ T cells and not with neutrophils in LUAD. Additionally, our results showed that SLC17A9 is related to innate immunity and adaptive immunity in LUAD.

Inhibitory immune checkpoint genes, such as PD-1 and its ligand (PDL1, PD-L2), CTLA-4, TIGIT, and TGFβ are important targets in the treatment of patients with NSCLC [9, 50, 51]. The immunoinhibitor genes are the most commonly used immune checkpoint, can be targeted by immunotherapies [50, 51]. Our study demonstrated that the expression level of SLC17A9 had a strong positive correlation with most immunoinhibitor (22/24) in LUSC, especially with A2aR, PD-1, CTLA-4, CSF1R, and TIGIT, which was also consistent with GSEA. Whereas a weaker positive correlation with a few markers exists in LUAD, such as A2aR, PD-1, CTLA-4, KIR2DL1, LAG3, TGFB1, TIGIT and B7-H4 in LUAD. Therefore, SLC17A9 may improve lung cancer patient prognosis through immune infiltration and activation. SLC17A9 could specially act as the promising target for clinical application of immunotherapy in LUSC. However, the role of SLC17A9 in the infiltration and activation of NK cells, macrophages and T cells in lung cancer is still controversial, and the exact role of SLC17A9 in the TME of LUAD and LUSC requires further investigation. LUAD and LUSC are distinct in disease pathology, molecular mechanisms, and immunogenic features. The influence of SLC17A9 in tumor immunity may be different between LUAD and LUSC. Although bioinformatics analysis is a powerful tool to highlight molecular mechanisms underlying SLC17A9, experimental validations are warranted to further validate our findings and explore the detailed mechanism at molecular and cellular levels.

It has been previously reported that SLC17A9 promoted proliferation in clear renal cell carcinoma [22] and prostate cancer [20]. SLC17A9 silencing reportedly inhibited the viability of C2C12, COS1, and HEK293T cells. Takai et al. [52] showed that TGF-β1 failed to induce release of ATP from SLC17A9-knockdown cells. Here, we demonstrated that SLC17A9 knockdown inhibited cell proliferation in A549 and H1299 cells by affecting MYC, cytochrome C, MFN2, and STAT3, and it also decreased the production of ATP by the P2X1 receptor. Although the mechanism underlying SLC17A9 regulation remains unknown, the present data strongly suggested that SLC17A9 potentially promotes the progression of LUAD and LUSC through its effects on the cell cycle, cell prolif-

eration, and DNA damage. ATP receptors such as P2RX1, P2RX7 and P2RX4 were significantly down-regulated in LUAD and LUSC. Collectively, we highlighted that SLC17A9 can be used as a prognostic marker and a potential therapeutic target for LUAD and LUSC.

Conclusion

By comprehensively analysis of the expression and prognostic significance of SLC17A family members, it reveals the importance of SLC17-A9 in LUAD and LUSC. Our current study represents the first comprehensive analysis for the relationship between SLC17A family and NSCLC progression. The crucial finding of our study was to identify a biomarker, we found that SLC17A9 was up-regulated and could be the promising diagnostic and prognostic biomarkers that associated with immune infiltration for patients with LUAD and LUSC. Additionally, we combined further bioinformatics and in vitro analyses to investigate the oncogenic function of SLC17A9. SLC17A9 might promote LUAD cell proliferation through regulating the expression of MYC and cytochrome C.

Acknowledgements

This work was supported by National Natural Science Foundation of China (No. 81971060), the Hubei Province's Outstanding Medical Academic Leader program, the Foundation for Innovative Research Team of Hubei Provincial Department of Education (No. T2020025), Free-exploring Foundation of Hubei University of Medicine (Grant No. FDFR201903), the Innovative Research Program for Graduates of Hubei University of Medicine (Grant No. YC2023007, YC2023035) and the Key Discipline Project of Hubei University of Medicine.

Disclosure of conflict of interest

None.

Address correspondence to: Zhijun Pei and Changbin Ke, Department of Nuclear Medicine and Institute of Anesthesiology and Pain, Taihe Hospital, Hubei University of Medicine, Shiyan 442000, Hubei, China. E-mail: pzjzml1980@taihehospital.com (ZJP); changbinke-iap@taihehospital.com (CBK)

References

[1] Siegel RL, Miller KD, Wagle NS and Jemal A. Cancer statistics, 2023. CA Cancer J Clin 2023; 73: 17-48.

[2] Altorki N, Villena-Vargas J and Wakelee H. Adjuvant therapy for early-stage non-small cell lung cancer: the breaking of a new dawn. J Thorac Cardiovasc Surg 2023; 165: 495-499.

[3] Zeng W, Zhao C, Yu M, Chen H, Pan Y, Wang Y, Bao H, Ma H and Ma S. Alterations of lung microbiota in patients with non-small cell lung cancer. Bioengineered 2022; 13: 6665-6677.

[4] Ma J, Chen X, Lin M, Wang Z, Wu Y and Li J. Bioinformatics analysis combined with experiments predicts CENPK as a potential prognostic factor for lung adenocarcinoma. Cancer Cell Int 2021; 21: 65.

[5] Wang J, Yuan Y, Tang L, Zhai H, Zhang D, Duan L, Jiang X and Li C. Long non-coding RNA-TMPO-AS1 as ceRNA binding to let-7c-5p upregulates STRIP2 expression and predicts poor prognosis in lung adenocarcinoma. Front Oncol 2022; 12: 921200.

[6] Byun DJ, Wolchok JD, Rosenberg LM and Girotra M. Cancer immunotherapy - immune checkpoint blockade and associated endocrinopathies. Nat Rev Endocrinol 2017; 13: 195-207.

[7] Hellmann MD, Nathanson T, Rizvi H, Creelan BC, Sanchez-Vega F, Ahuja A, Ni A, Novik JB, Mangarin LMB, Abu-Akeel M, Liu C, Sauter JL, Rekhtman N, Chang E, Callahan MK, Chaft JE, Voss MH, Tenet M, Li XM, Covello K, Renninger A, Vitazka P, Geese WJ, Borghaei H, Rudin CM, Antonia SJ, Swanton C, Hammerbacher J, Merghoub T, McGranahan N, Snyder A and Wolchok JD. Genomic features of response to combination immunotherapy in patients with advanced non-small-cell lung cancer. Cancer Cell 2018; 33: 843-852, e4.

[8] Zeng Z, Yang F, Wang Y, Zhao H, Wei F, Zhang P, Zhang X and Ren X. Significantly different immunological score in lung adenocarcinoma and squamous cell carcinoma and a proposal for a new immune staging system. Oncoimmunology 2020; 9: 1828538.

[9] Bogart JA. Immune checkpoint inhibition for locally advanced NSCLC: time to ask new questions? J Thorac Oncol 2022; 17: 1330-1332.

[10] Kargl J, Zhu X, Zhang H, Yang GHY, Friesen TJ, Shipley M, Maeda DY, Zebala JA, McKay-Fleisch J, Meredith G, Mashadi-Hossein A, Baik C, Pierce RH, Redman MW, Thompson JC, Albelda SM, Bolouri H and Houghton AM. Neutrophil content predicts lymphocyte depletion and anti-PD1 treatment failure in NSCLC. JCI Insight 2019; 4: e130850.

[11] Zhang Q, Bi J, Zheng X, Chen Y, Wang H, Wu W, Wang Z, Wu Q, Peng H, Wei H, Sun R and Tian Z. Blockade of the checkpoint receptor TIGIT prevents NK cell exhaustion and elicits potent anti-tumor immunity. Nat Immunol 2018; 19: 723-732.

[12] Reimer RJ. SLC17: a functionally diverse family of organic anion transporters. Mol Aspects Med 2013; 34: 350-359.

[13] Cao Q, Zhao K, Zhong XZ, Zou Y, Yu H, Huang P, Xu T and Dong XP. SLC17A9 protein functions as a lysosomal ATP transporter and regulates cell viability. J Biol Chem 2014; 289: 23189-23199.
[14] Mihara H, Uchida K, Koizumi S and Moriyama Y. Involvement of VNUT-exocytosis in transient receptor potential vanilloid 4-dependent ATP release from gastrointestinal epithelium. PLoS One 2018; 13: e0206276.
[15] Inoue A, Nakao-Kuroishi K, Kometani-Gunjigake K, Mizuhara M, Shirakawa T, Ito-Sago M, Yasuda K, Nakatomi M, Matsubara T, Tada-Shigeyama Y, Morikawa K, Kokabu S and Kawamoto T. VNUT/SLC17A9, a vesicular nucleotide transporter, regulates osteoblast differentiation. FEBS Open Bio 2020; 10: 1612-1623.
[16] Kui XY, Gao Y, Liu XS, Zeng J, Yang JW, Zhou LM, Liu XY, Zhang Y, Zhang YH and Pei ZJ. Comprehensive analysis of SLC17A9 and its prognostic value in hepatocellular carcinoma. Front Oncol 2022; 12: 809847.
[17] Wu J, Yang Y and Song J. Expression of SLC17A9 in hepatocellular carcinoma and its clinical significance. Oncol Lett 2020; 20: 182.
[18] Yang L, Chen Z, Xiong W, Ren H, Zhai E, Xu K, Yang H, Zhang Z, Ding L, He Y, Song X and Liu J. High expression of SLC17A9 correlates with poor prognosis in colorectal cancer. Hum Pathol 2019; 84: 62-70.
[19] Li J, Su T, Yang L, Deng L, Zhang C and He Y. High SLC17A9 expression correlates with poor survival in gastric carcinoma. Future Oncol 2019; 15: 4155-4166.
[20] Mi YY, Sun CY, Zhang LF, Wang J, Shao HB, Qin F, Xia GW and Zhu LJ. Long non-coding RNAs LINC01679 as a competitive endogenous RNAs inhibits the development and progression of prostate cancer via regulating the miR-3150a-3p/SLC17A9 axis. Front Cell Dev Biol 2021; 9: 737812.
[21] Meng M, Lan T, Tian D, Qin Z, Li Y, Li J and Cao H. Integrative bioinformatics analysis demonstrates the prognostic value of chromatin accessibility biomarkers in clear cell renal cell carcinoma. Front Oncol 2021; 11: 814396.
[22] Li W, Xu N, Meng X, Yuan H, Yu T, Miao Q, Yang H, Hai B, Xiao W and Zhang X. SLC17A9-PTHLH-EMT axis promotes proliferation and invasion of clear renal cell carcinoma. Iscience 2022; 26: 105764.
[23] Tokunaga A, Tsukimoto M, Harada H, Moriyama Y and Kojima S. Involvement of SLC17A9-dependent vesicular exocytosis in the mechanism of ATP release during T cell activation. J Biol Chem 2010; 285: 17406-17416.
[24] Mihara H, Boudaka A, Tominaga M and Sugiyama T. Transient receptor potential vanilloid 4 regulation of adenosine triphosphate release by the adenosine triphosphate transporter vesicular nucleotide transporter, a novel therapeutic target for gastrointestinal baroreception and chronic inflammation. Digestion 2020; 101: 6-11.
[25] Galensa K. ggplot2: elegant graphics for data analysis (2nd ed.). Computing Reviews 2017.
[26] Gao J, Aksoy BA, Dogrusoz U, Dresdner G, Gross B, Sumer SO, Sun Y, Jacobsen A, Sinha R, Larsson E, Cerami E, Sander C and Schultz N. Integrative analysis of complex cancer genomics and clinical profiles using the cBioPortal. Sci Signal 2013; 6: pl1.
[27] Nagy Á, Munkácsy G and Győrffy B. Pancancer survival analysis of cancer hallmark genes. Sci Rep 2021: 11: 6047.
[28] Vasaikar SV, Straub P, Wang J and Zhang B. LinkedOmics: analyzing multi-omics data within and across 32 cancer types. Nucleic Acids Res 2018; 46: D956-D963.
[29] Szklarczyk D, Franceschini A, Kuhn M, Simonovic M, Roth A, Minguez P, Doerks T, Stark M, Muller J, Bork P, Jensen LJ and von Mering C. The STRING database in 2011: functional interaction networks of proteins, globally integrated and scored. Nucleic Acids Res 2011; 39: D561-D568.
[30] Li T, Fan J, Wang B, Traugh N, Chen Q, Liu JS, Li B and Liu XS. TIMER: a web server for comprehensive analysis of tumor-infiltrating immune cells. Cancer Res 2017; 77: e108-e110.
[31] Lee C, Park J, Oh JI, Kim B, Kwon JH, Kim BK, Ahn K and Yoon S. Abstract 3540: down-regulation of solute carrier family 17 member 1(SLC17A1) expression contributes to chemotherapy resistance in acute myeloid leukemia. Cancer Res (Chicago, Ill.) 2010; 70: 3540.
[32] Devarakonda S, Rotolo F, Tsao MS, Lanc I, Brambilla E, Masood A, Olaussen KA, Fulton R, Sakashita S, Mcleer-Florin A, Ding K, Le Teuff G, Shepherd FA, Pignon JP, Graziano SL, Kratzke R, Soria JC, Seymour L, Govindan R and Michiels S. Tumor mutation burden as a biomarker in resected non-small-cell lung cancer. J Clin Oncol 2018; 36: 2995-3006.
[33] Sakashita S, Masahiro M, Matsuoka R, Muratani M and Noguchi M. P1.09-16 novel somatic gene mutation of SLC17A9, detected in early-stage lung adenocarcinoma. J Thorac Oncol 2018; 13: S556.
[34] Herbst RS, Morgensztern D and Boshoff C. The biology and management of non-small cell lung cancer. Nature 2018; 553: 446-454.
[35] Lord CJ and Ashworth A. The DNA damage reponse and cancer therapy. Nature 2012; 481: 287-294.
[36] Sanchez-Vega F, Mina M, Armenia J, Chatila WK, Luna A, La KC, Dimitriadoy S, Liu DL, Kantheti HS, Saghafinia S, Chakravarty D, Daian F, Gao Q, Bailey MH, Liang WW, Foltz SM, Shmu-

levich I, Ding L, Heins Z, Ochoa A, Gross B, Gao J, Zhang H, Kundra R, Kandoth C, Bahceci I, Dervishi L, Dogrusoz U, Zhou W, Shen H, Laird PW, Way GP, Greene CS, Liang H, Xiao Y, Wang C, Iavarone A, Berger AH, Bivona TG, Lazar AJ, Hammer GD, Giordano T, Kwong LN, McArthur G, Huang C, Tward AD, Frederick MJ, McCormick F, Meyerson M; Cancer Genome Atlas Research Network, Van Allen EM, Cherniack AD, Ciriello G, Sander C and Schultz N. Oncogenic signaling pathways in the cancer genome atlas. Cell 2018; 173: 321-337, e10.

[37] Gupta S, Silveira DA and Mombach JCM. Towards DNA-damage induced autophagy: a boolean model of p53-induced cell fate mechanisms. Dna Repair (Amst) 2020; 96: 102971.

[38] Hasuzawa N, Moriyama S, Moriyama Y and Nomura M. Physiopathological roles of vesicular nucleotide transporter (VNUT), an essential component for vesicular ATP release. Biochim Biophys Acta Biomembr 2020; 1862: 183408.

[39] Schenk U, Frascoli M, Proietti M, Geffers R, Traggiai E, Buer J, Ricordi C, Westendorf AM and Grassi F. ATP inhibits the generation and function of regulatory t cells through the activation of purinergic P2X receptors. Sci Signal 2011; 4: ra12.

[40] Zhong XZ, Cao Q, Sun X and Dong XP. Activation of lysosomal P2X4 by ATP transported into lysosomes via VNUT/SLC17A9 using V-ATPase generated voltage gradient as the driving force. J Physiol 2016; 594: 4253-4266.

[41] Rivera A, Vanzulli I and Butt AM. A central role for ATP signalling in glial interactions in the CNS. Curr Drug Targets 2016; 17: 1829-1833.

[42] Yegutkin GG and Boison D. ATP and adenosine metabolism in cancer: exploitation for therapeutic gain. Pharmacol Rev 2022; 74: 799-824.

[43] Di Virgilio F, Vultaggio-Poma V and Sarti AC. P2X receptors in cancer growth and progression. Biochem Pharmacol 2021; 187: 114350.

[44] Gu LQ, Li FY, Zhao L, Liu Y, Chu Q, Zang XX, Liu JM, Ning G and Zhao YJ. Association of XIAP and P2X7 receptor expression with lymph node metastasis in papillary thyroid carcinoma. Endocrine 2010; 38: 276-282.

[45] Adinolfi E, Capece M, Amoroso F, De Marchi E and Franceschini A. Emerging roles of P2X receptors in cancer. Curr Med Chem 2015; 22: 878-90.

[46] Sheng W, LaFleur MW, Nguyen TH, Chen S, Chakravarthy A, Conway JR, Li Y, Chen H, Yang H, Hsu PH, Van Allen EM, Freeman GJ, De Carvalho DD, He HH, Sharpe AH and Shi Y. LSD1 ablation stimulates anti-tumor immunity and enables checkpoint blockade. Cell 2018; 174: 549-563, e19.

[47] Duan Z and Ho M. T-cell receptor mimic antibodies for cancer immunotherapy. Mol Cancer Ther 2021; 20: 1533-1541.

[48] Lang PA, Merkler D, Funkner P, Shaabani N, Meryk A, Krings C, Barthuber C, Recher M, Brück W, Häussinger D, Ohashi PS and Lang KS. Oxidized ATP inhibits T-cell-mediated autoimmunity. Eur J Immunol 2010; 40: 2401-2408.

[49] Ledderose C, Bromberger S, Slubowski CJ, Sueyoshi K, Aytan D, Shen Y and Junger WG. The purinergic receptor P2Y11 choreographs the polarization, mitochondrial metabolism, and migration of T lymphocytes. Sci Signal 2020; 13: eaba3300.

[50] Kraehenbuehl L, Weng CH, Eghbali S, Wolchok JD and Merghoub T. Enhancing immunotherapy in cancer by targeting emerging immunomodulatory pathways. Nat Rev Clin Oncol 2022; 19: 37-50.

[51] Mahoney KM, Rennert PD and Freeman GJ. Combination cancer immunotherapy and new immunomodulatory targets. Nat Rev Drug Discov 2015; 14: 561-584.

[52] Takai E, Tsukimoto M, Harada H, Sawada K, Moriyama Y and Kojima S. Autocrine regulation of TGF-β1-induced cell migration by exocytosis of ATP and activation of P2 receptors in human lung cancer cells. J Cell Sci 2012; 125: 5051-5060.

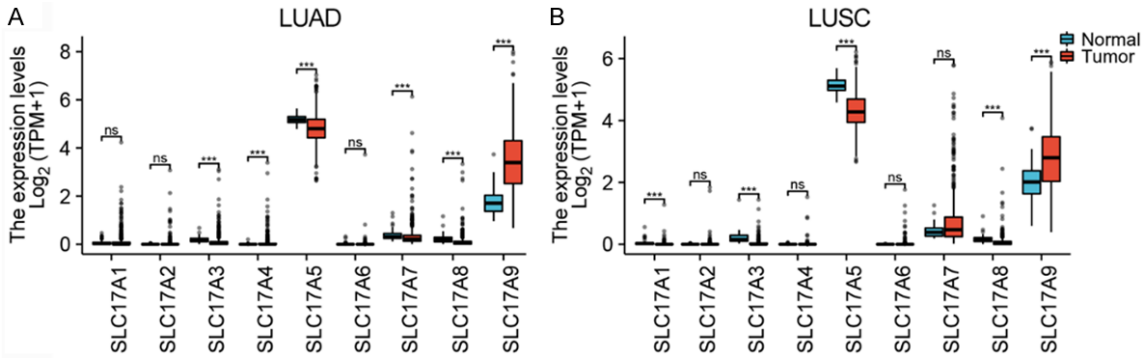

Figure S1. Expression and overall survival characteristics of SLC17As in human LUAD and LUSC tissues. A. Relative mRNA levels of nine SLC17As across tumor tissues (N = 510) and normal tissues (N = 59) in LUAD were analyzed using TCGA databases, TPM, transcripts per million reads. B. Relative mRNA levels of nine SLC17As across tumor tissues (N = 546) and normal tissues (N = 57) in LUSC were analyzed using TCGA databases. The t-test was used to estimate the significance of difference in gene expression levels between groups, ns, *$P < 0.05$; **$P < 0.01$; ***$P < 0.001$.

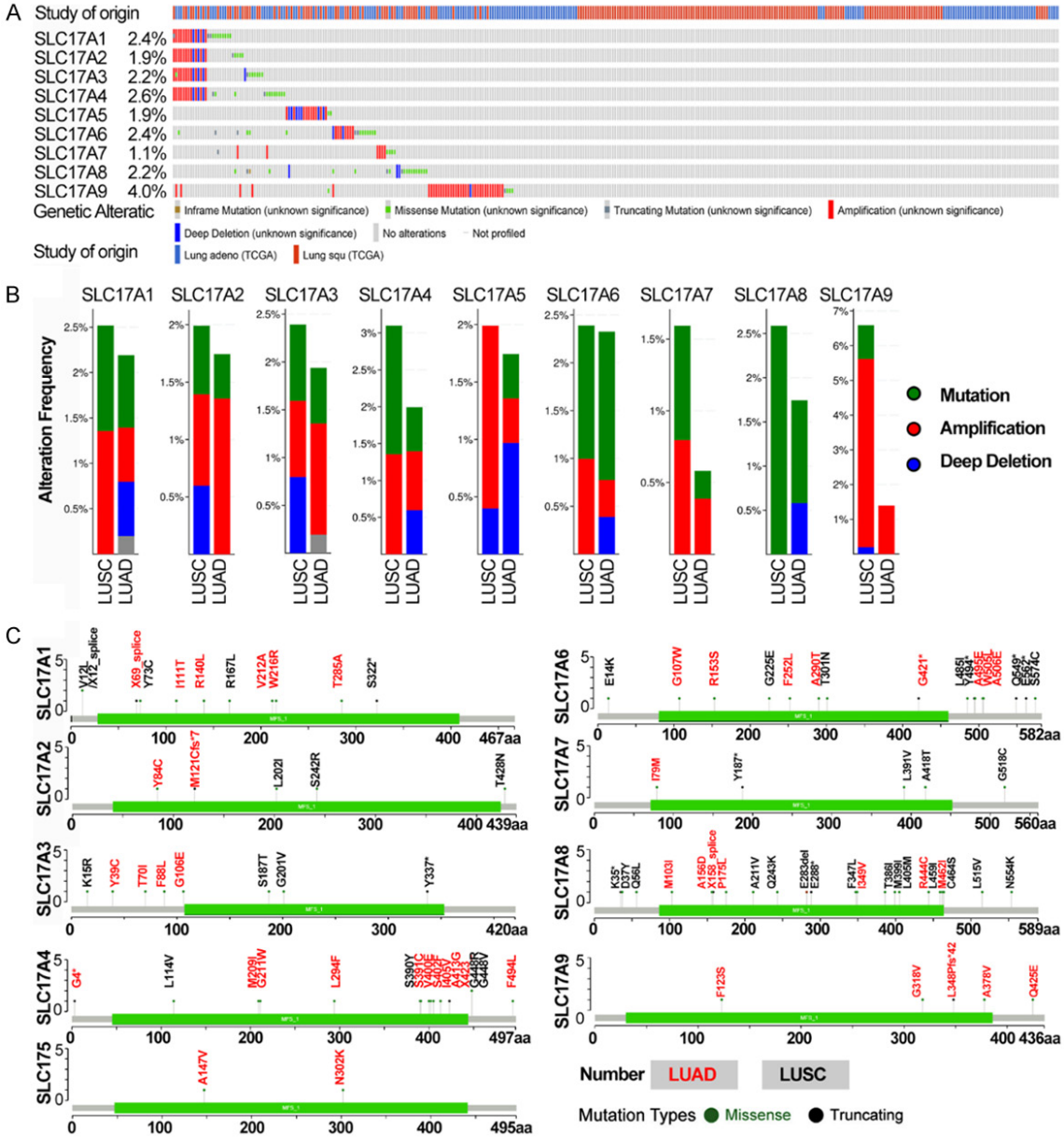

Figure S2. Summary of genetic mutations in SLC17A family genes in LUAD and LUSC by cBioPortal. A. The total alteration of frequency were colored by the type in LUAD and LUSC studies. B. The mutation profile and putative copy-number alterations (CNAs) represented as columns in TCGA cohort. C. The structured domains and the location of fragments of SLC17As mutations in LUAD and LUSC.

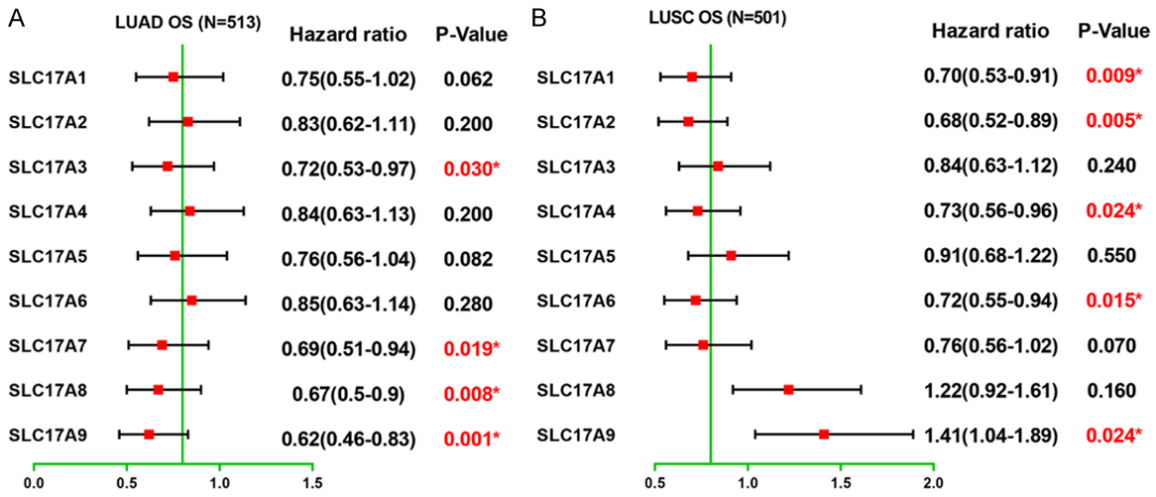

Figure S3. Forest plot of hazard ratios depicting overall survival (OS) of SLC17A genes in LUAD (A) and LUSC (B) (red values $*P < 0.05$).

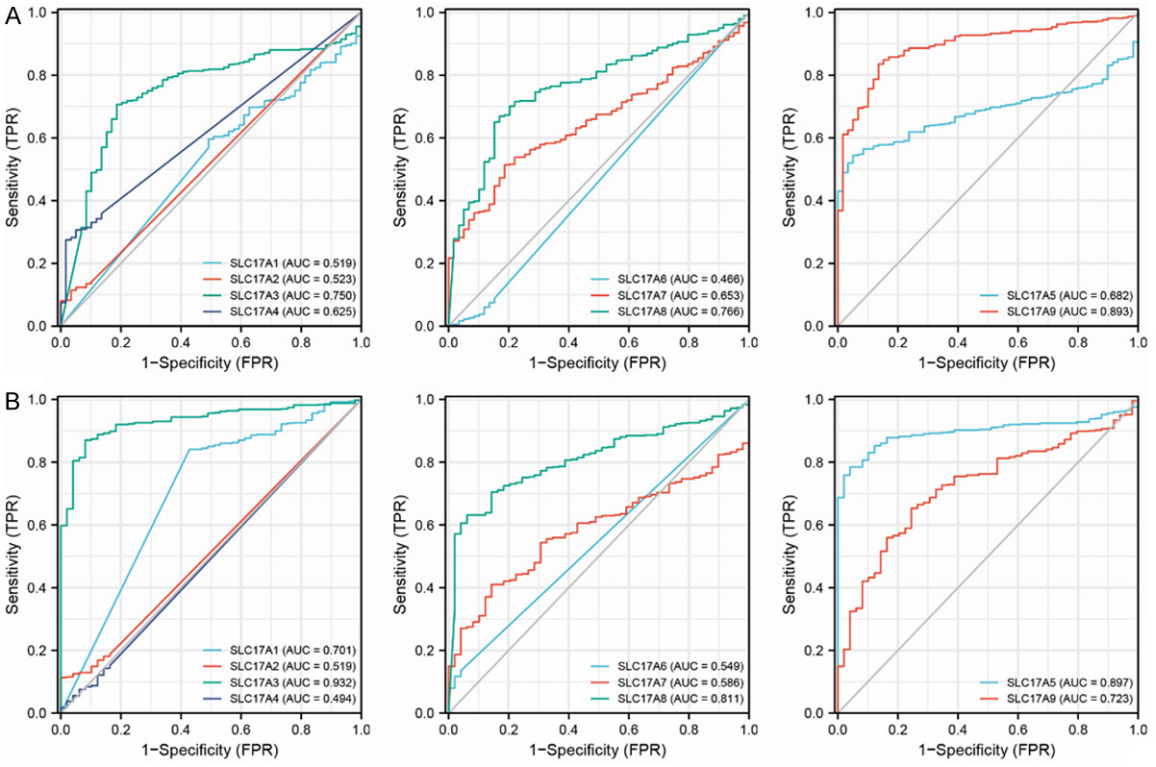

Figure S4. The ROC curve of individual SLC17A family genes including type I phosphate transporters (SLC17A1/2/3/4), vesicular glutamate transporters (SLC17A6/7/8), SLC17A5 and SLC17A9 in patients with LUAD (A) and LUSC (B), TPR, true positive ratio, FPR, false positive ratio. $0.5 < AUC \leq 0.7$ implicated less predictive, $0.7 < AUC \leq 0.9$ indicated moderately predictive and $0.9 < AUC < 1$ referred to highly predictive.

Table S1. The association between SLC17A9 mRNA levels and clinical-pathological characteristics of LUAD and LUSC patients in TCGA

Characteristic	LUAD			LUSC		
	Low	High	*P*	Low	High	*P*
n	267	268		251	251	
Age, meidan (IQR)	67 (60, 72)	65 (58, 72)	0.294	67 (62, 73)	69 (62, 74)	0.258
Gender, n (%)			0.968			0.839
Female	142 (26.5%)	144 (26.9%)		64 (12.7%)	67 (13.3%)	
Male	125 (23.4%)	124 (23.2%)		187 (37.3%)	184 (36.7%)	
Age, n (%)			0.656			0.438
≤ 65	122 (23.6%)	133 (25.8%)		100 (20.3%)	91 (18.5%)	
> 65	131 (25.4%)	130 (25.2%)		146 (29.6%)	156 (31.6%)	
T stage, n (%)			0.947			0.170
T1, 2	230 (43.3%)	234 (43.9%)		210 (41.9%)	198 (39.5%)	
T3, 4	34 (6.4%)	34 (6.4%)		41 (8.2%)	53 (10.6%)	
N stage, n (%)			0.386			0.861
N0	165 (31.8%)	183 (35.3%)		161 (32.5%)	159 (32.1%)	
N1-3	88 (17.0%)	83 (16.0%)		90 (18.1%)	86 (17.3%)	
M stage, n (%)			0.142			0.721
M0	183 (47.4%)	178 (46.1%)		209 (49.9%)	203 (48.4%)	
M1	17 (4.4%)	8 (2.1%)		3 (0.7%)	4 (1%)	
pStage, n (%)			0.704			0.474
Stage I	144 (27.3%)	150 (28.5%)		126 (25.3%)	119 (23.9%)	
Stage II-IV	118 (22.4%)	115 (21.8%)		122 (24.5%)	131 (26.3%)	